TAR DNA-binding Protein 43 as a Damage-associated Molecular Pattern in Amyotrophic Lateral Sclerosis-related Neuroinflammation

Doctoral thesis

to obtain a doctorate

from the Faculty of Medicine

of the University of Bonn

<u>Tizian</u> Keno Meyer

from Freiburg im Breisgau

2024

Written with authorization of

the Faculty of Medicine of the University of Bonn

First reviewer: PD Dr. med. Patrick Weydt

Second reviewer: Prof. Dr. med. Matthias Geyer

Day of oral examination: 19.12.2023

From the Clinic for Neurodegenerative Diseases and Geriatric Psychiatry

Director: Prof. Dr. med. Ullrich Wüllner

Table of contents

List of abbreviations

AD	Alzheimer's Disease
ANOVA	Analysis of Variance
ASC	Apoptosis-associated Speck-like Protein Containing a CARD
BMDM	Bone Marrow-derived Macrophage
BSA	Bovine Serum Albumin
C9ORF72	Chromosome 9 Open Reading Frame 72
CD	Cluster of Differentiation
CNS	Central Nervous System
CRID3	Cytokine Release Inhibitory Drug 3
CSF	Cerebrospinal Fluid
CTF	C-terminal Fragment
CXCL	C-X-C Motif Chemokine Ligand
DAMP	Damage-associated Molecular Pattern
DAPI	4′,6-Diamidino-2-Phenylindole
DMEM	Dulbecco's Modified Eagle's Medium
DPBS	Dulbecco's Phosphate Buffered Saline
DPR	Dipeptide Repeat
ELISA	Enzyme-linked Immunosorbent Assay
FLICA	Fluorochrome-Labeled Inhibitors of Caspases
FTD	Frontotemporal Dementia
fTDP	Fibrillary TDP-43 Protein
FTLD-U	Frontotemporal Lobar Degeneration with Ubiquitin-positive Inclusions
FUS	Fused in Sarcoma
G-CSF	Granulocyte Colony-stimulating Factor
GA	Glycine-Alanine
GM-CSF	Granulocyte-Macrophage Colony-stimulating Factor
GP	Glycine-Proline
GR	Glycine-Arginine

hMDM	Human Monocyte-derived Macrophage
hnRNP	Heterogeneous Nuclear Ribonucleoprotein
Iba-1	Ionized Calcium-binding Adaptor Molecule 1
iFBS	Inactivated Fetal Bovine Serum
IFM	IFM-2384
IL	Interleukin
LATE	Limbic-predominant Age-related TDP-43 Encephalopathy
LDH	Lactate Dehydrogenase
LLPS	Liquid-liquid Phase Separation
LMN	Lower Motor Neuron
LPS	Lipopolysaccharide
MCC950	see CRID3
MND	Motor Neuron Disease
MPS	Mononuclear Phagocytic System
mTDP	Monomeric TDP-43 Protein
MTT	3-[4,5-Dimethylthiazol-2-yl]-2,5 Diphenyl Tetrazolium Bromide
NDS	Normal Donkey Serum
NF-κB	Nuclear Factor 'Kappa-light-chain-enhancer' of Activated B-cells
NLRP3	NOD-, LRR- and Pyrin Domain-containing 3
P/S	Penicillin/Streptomycin
PAMP	Pathogen-associated Molecular Pattern
PA	Proline-Alanine
PBP	Progressive Bulbar Palsy
PD	Parkinson's Disease
PE	Phycoerythrin
PI	Propidium Iodide
PLS	Primary Lateral Sclerosis
PMA	Progressive Muscular Atrophy
PMG	Primary Microglia
PR	Proline-Arginine
PRR	Pattern Recognition Receptor

PTM	Posttranslational Modification
RAN	Repeat-associated non-ATG
RIPA	Radioimmunoprecipitation Assay
SDS	Sodium Dodecyl Sulfate
SEM	Standard Error of the Mean
sICAM	Soluble Intercellular Adhesion Molecule 1
SOD1	Superoxide Dismutase
TBST	Tris-buffered Saline Supplemented with Tween-20
TDP-43	TAR DNA-binding Protein 43
TEM	Transmission Electron Microscope
TIMP	Tissue Inhibitor of Metalloproteinase
TLR	Toll-like Receptor
TNF-α	Tumor Necrosis Factor α
UMN	Upper Motor Neuron
XTT	2,3-Bis-(2-Methoxy-4-Nitro-5-Sulfophenyl)-2H-Tetrazolium-5-Carboxanilide

1. Introduction

1.1 Amyotrophic Lateral Sclerosis

1.1.1 Overview

Amyotrophic lateral sclerosis (ALS), in the United States also known as Lou Gehrig's disease, was first described by Jean-Martin Charcot in the year 1869 and is nowadays the most common form of adult-onset motor neuron degeneration. The disease is hallmarked by a demise of neurons in the brain and its descending axons in the corticospinal tract as well as spinal motor neurons, which ultimately leads to muscle atrophy caused by secondary denervation. Gradually increasing muscle weakness is the most prominent feature of clinical manifestations which show a relentlessly progressing character often culminating in respiratory failure. Although efforts made to unravel the pathogenesis of the disease have been immense, fundamental aspects of driving mechanisms still remain enigmatic. This also accounts for the fact that no therapy with a striking effect has yet been established and only a few drugs with mainly symptomatic effects are in use. Considering the urgent need for a better understanding of disease pathology, it is of great importance to extend the existing knowledge and develop the basis for future therapeutic options.

1.1.2 Epidemiology

In comparison to other major neurodegenerative diseases like Alzheimer's disease (AD) and Parkinson's disease (PD), case numbers of ALS are relatively low with an overall incidence of 0.6 - 3.8 cases per year per 100,000 individuals and a prevalence of 4.1 - 8.4 per 100,000 people (Longinetti and Fang, 2019). Therefore, ALS is mostly described as a rare disease, which is consistent with the definition within the European Union that considers diseases below a prevalence of 1 in 2000 people to be "rare" (Moliner and Waligora, 2017). Nonetheless, the cross-gender lifetime risk of ALS is 1:400 (Ryan et al., 2019). This can be explained by an extremely short average time of survival with 24 to 50 months, which leads to a prevalence that only marginally exceeds disease incidence (Longinetti

and Wang, 2019). Men are affected more often and at a younger age than women (1.1 - 3:1) and most patients are diagnosed at an advanced age, with a maximum at approximately 62-67 years (Cacabelos et al., 2016; Chiò et al., 2013; Logroscino et al., 2010; Uenal et al., 2014). The majority of disease cases occur isolated in nature and are considered "sporadic", while about 5-10 % have a clear family history (Talbott et al., 2016).

1.1.3 Pathophysiology

Overall, a clear understanding of disease mechanisms remains elusive. At the molecular level, a broad variety of underlying mechanisms were identified that drive disease onset and progression. Key contributors implicated in these processes are altered RNA metabolism, disturbed protein homeostasis and non-cell autonomous toxicity (Taylor et al., 2016). In addition, an extensive number of genetic factors were identified to be associated with the disease during the last decades.

One seminal finding was made in 2006, where TAR-DNA-binding protein 43 (TDP-43) was identified as the major component of neuronal inclusions in up to 97 % of sporadic and also some familial ALS cases (Arai et al., 2006; Neumann et al., 2006). This groundbreaking discovery was essential not only for a better understanding of ALS pathophysiology but established a molecular link between sporadic and familial ALS forms. Besides *post-mortem* tissue from ALS patients, aggregated TDP-43 protein was found in sporadic and familial frontotemporal lobar degeneration with ubiquitin-positive inclusions (FTLD-U), the most common subtype of frontotemporal dementia (FTD) (Neumann et al., 2006). This underlined the pivotal role of TDP-43 in neurodegeneration and provided a molecular basis for the partial clinical overlap of ALS and FTD. Moreover, recent research has discovered TDP-43-positive inclusions in other neurodegenerative diseases like Alzheimer's or Parkinson's disease (Chanson et al., 2010; Lippa et al., 2009). To account for the plethora of diseases involved in TDP-43 pathology, the term TDP-43 proteinopathy has been introduced and even recently recognized disease entities like limbic-predominant age-related TDP-43 encephalopathy (LATE) are named after this protein (Nelson et al., 2019).

For familial ALS-cases, a scientific milestone was the detection of an expanded GGGGCC (G_4C_2) hexanucleotide repeat in the first intron of *chromosome 9 open reading frame 72 (C9ORF72)* in 2011 (DeJesus-Hernandez et al., 2011; Renton et al., 2011). Normally the maximum size of these repeats reaches a length of 23 units whereas in affected individuals it can expand to sizes of multiple hundreds and even thousands. This enlarged sequence leads to the generation of five distinct secondary-derived dipeptide repeats (DPRs) via an unusual repeat-associated non-ATG (RAN) translation of sense and antisense *C9ORF72*-transcripts (Mori et al., 2013). This unconventional form of translation is initiated in the absence of an AUG codon and is probably due to secondary, hairpin-like structures formed by the expanded repeats (Zu et al., 2011). The five resulting dipeptides are proline-alanine (PA), proline-arginine (PR), glycine-alanine (GA), glycine-arginine (GR) and glycine-proline (GP). Especially the arginine-containing DPRs PR and GR possess toxic properties and are known to interfere with RNA processing (Lee et al., 2016). The detrimental effect of these peptides is still not fully understood, yet there is evidence that the *C9ORF72*-related subtype is the most common form of familial ALS cases with an overall proportion of about 40 % (Pliner et al., 2014).

Besides an altered *C9ORF72*-gene, a broad variety of genetic mutations are known to cause familial ALS. In 1993, the first discovery was a mutation in the *SOD1* gene, which encodes for a cytosolic, Cu/Zn-binding superoxide dismutase (Rosen et al., 1993). It physiologically converts the toxic superoxide anion O^-_2 to O_2 and H_2O_2 and is linked to free radical toxicity. The identification of many other mutations in ALS-related genes followed, with the most important ones being *fused in sarcoma (FUS)* and the already described *TAR DNA-binding protein 43 (TARDBP)* (Gitcho et al., 2008; Kabashi et al., 2008; Lattante et al., 2013; Sreedharan et al., 2008; T. J. Kwiatkowski et al., 2009; Vance et al., 2009). These findings underpinned the significance of a disturbed RNA metabolism in ALS pathophysiology, as both of the encoded proteins, together with some lesser-known examples, belong to the family of heterogeneous nuclear ribonucleoproteins (hnRNPs). Members of this protein family are able to interact with the RNA life cycle at basically all stages, thus impairment of their normal function results in a large range of potential complications (Lagier-Tourenne et al., 2012). Another shared hallmark of these nuclear proteins is the presence of low-complexity domains in their respective C-terminal regions. This enables them to interfere with each other and rearrange themselves in membrane-less granule-

like compartments, a biochemical process which is known as liquid-liquid phase separation (LLPS) (Molliex et al., 2015). The same process occurs during the formation of stress granules, subcellular compartments that are built in critical metabolic states and are hypothesized to be of special impact for the pathogenesis of neurodegenerative diseases including ALS (Li et al., 2013).

1.1.4 Clinical manifestations and classification

The defining pathological feature of ALS is the progressive loss of upper and lower motor neurons resulting clinically in a rapid and relentless decline of muscular functions. The distribution of affected motor neurons can vary and shows an overlap with other debilitating diseases, all of which can be termed motor neuron diseases (MNDs). ALS makes up for 80-90 % of MND cases, yet the different entities are difficult to distinguish, complicated by the fact that ALS is mainly a clinical diagnosis (Yedavalli et al., 2018). In the classical form of ALS, signs of an impaired first and second motor neuron are both prevalent, with mainly innocuous initial symptoms like asymmetric distal limb weakness, muscle cramps or slurred and nasal speech. Besides gradually increasing muscle weakness as the most prominent feature of ALS, a subset of patients can suffer from cognitive impairment and executive dysfunction, as well as behavioral changes. An important criterion for the distinction of these subtypes is their discriminative impairment of the primary and secondary motor neuron. On the one hand, this includes primary lateral sclerosis (PLS) with pure upper motor neuron (UMN) degeneration and progressive muscular atrophy (PMA) with isolated affection of the lower motor neuron (LMN). Located between these two forms is UMN-predominant ALS where also signs of LMN-degeneration are prevalent. On the other hand, regional distribution of involvement may vary, primarily affecting regions like the brain stem or the diaphragm (Masrori and Van Damme, 2020). As already mentioned, cognitive impairment is a common symptom for patients suffering from ALS, as mild cognitive impairment can be found in about 50 % of cases (Mackenzie, 2007). On top of that, more severe dysfunctions, reaching the criteria for FTD, occur in as many as 10-15 %. Conversely, approximately 15 % of FTD patients show characteristics of motor neuron dysfunction (Ringholz et al., 2005). This overlap, as well as the fact that TDP-43-positive inclusions can be found in both ALS and FTD, established not only a clinical but also a

molecular connection between these two diseases entities. Therefore, ALS with fronto-temporal dementia (ALS-FTD) as a specific subtype combining extra-motor manifestations like behavioral and cognitive deficits is increasingly recognized (Liscic et al., 2020).

1.1.5 Diagnosis

ALS is a clinical diagnosis. Several scores have been established to simplify and stand-ardize diagnosis and a variety of diagnostic techniques help to diagnose ALS patients (Ludolph et al., 2021). These include electromyography (EMG), laboratory analysis of samples from blood or cerebrospinal fluid, magnetic resonance imaging (MRI) and genetic testing. Since none of these methods are fully specific, early symptoms of ALS can be ambiguous and a variety of ALS mimics and subtypes exist, a definite diagnosis is often delayed (Nzwalo et al., 2014).

While elevated concentrations of TDP-43 can be detected in cerebrospinal fluid (CSF) of ALS patients, high protein levels could serve as a useful marker of the disease, similar to β-amyloid and tau protein in AD (Lee et al., 2019; Olsson et al., 2016; Vu and Bowser, 2017). Elevated levels of TDP-43 protein were also found in the plasma of ALS-affected individuals (Ren et al., 2021; Verstraete et al., 2012). However, several open questions remain and future research is necessary (Verber and Shaw, 2020).

1.1.6 Treatment options

Disease modifying treatment options for ALS remain unsatisfactory and represent an important unmet need in the therapy of the disease (Ludolph et al., 2021). Riluzole, an antiglutamatergic substance which is thought to reduce excitotoxicity, is the only approved pharmaceutical drug capable to significantly ameliorate disease progression (Andrews et al., 2020; Miller et al., 2012). The effects of the antioxidant edaravone remain controversial, thus the drug has no approval for the European Union (Abe et al., 2014; Writing Group et al., 2017).

Throughout the last decade, this limitation of treatment options resulted in an increasing investment of scientific resources by pharmaceutical companies into the development of new therapeutic options. By the end of 2021 over 120 clinical trials for potential ALS-drugs were ongoing, with 18 different agents tested in phase III (Global Data Plc, 2022). Despite these intensified efforts, the overwhelming majority of drugs demonstrated no significant clinical efficacy (Petrov et al., 2017). The effects shown by the newly developed compounds are usually only symptomatic and do not modify the course of ALS. Many promising agents aim to mitigate neuronal cell death or prevent neuroinflammatory reactions, while some strategies like autologous stem cell therapy with mesenchymal stromal cells (MSCs) or treatment with antisense oligonucleotides (ASOs) try to intervene on a genetic level (Oskarsson et al., 2018). Future clinical trials will reveal if these novel methods have a significant effect also for ALS pathology. Besides the urgent need of an effective treatment for current ALS patients, the importance of further research is strengthened by the fact that future case numbers are likely to rise due to a globally ageing population. Estimations project a rise of nearly 70 % until 2040, stating that continuously improving health care systems and better diagnosis standards could lead to even higher numbers (Arthur et al., 2016). For all the stated reasons it is mandatory to achieve a more profound understanding of ALS as a disease.

1.2 TAR DNA-binding Protein 43 (TDP-43)

TDP-43 protein is a highly conserved and widely expressed nuclear factor, which has a length of 414 amino acids and consists of two RNA recognition motifs and a glycine-rich C-terminal region (Ince et al., 2011; Kato et al., 2012). This C-terminal region acts as a low-complexity domain, thus interacting with various nuclear acids and proteins, a typical feature of proteins that belong to the group of hnRNPs (Lagier-Tourenne et al., 2012; Molliex et al., 2015). Under normal conditions TDP-43 is mainly a nuclear protein that, to some extent, shuttles between the cytoplasm and the nucleus (Ayala et al., 2008). In pathological state, this homeostasis is disturbed resulting in redistribution of TDP-43 predominantly to the cytoplasm and neurites of affected cells, where aggregates of mainly full-length and often ubiquitinated and fragmented protein are formed (Barmada et al., 2010). Besides this sole deposition of misfolded protein aggregates, an often prion-like

propagation of these same aggregates throughout the central nervous system (CNS) is postulated, commonly termed "seeding". Here, mostly insoluble and aberrantly aggregated protein species gain pathological properties to seed cytosolic aggregation and cell-to-cell transmissibility, which in turn leads to disease progression to primarily unaffected regions within the neuronal network (Nonaka et al., 2013; Walker et al., 2013). As a relevant part of the TDP-43 protein consists of low-complexity domains, it is not surprising that TDP-43 is capable to induce seeding in a template-dependent manner (Furukawa et al., 2011; Maniecka and Polymenidon, 2015).
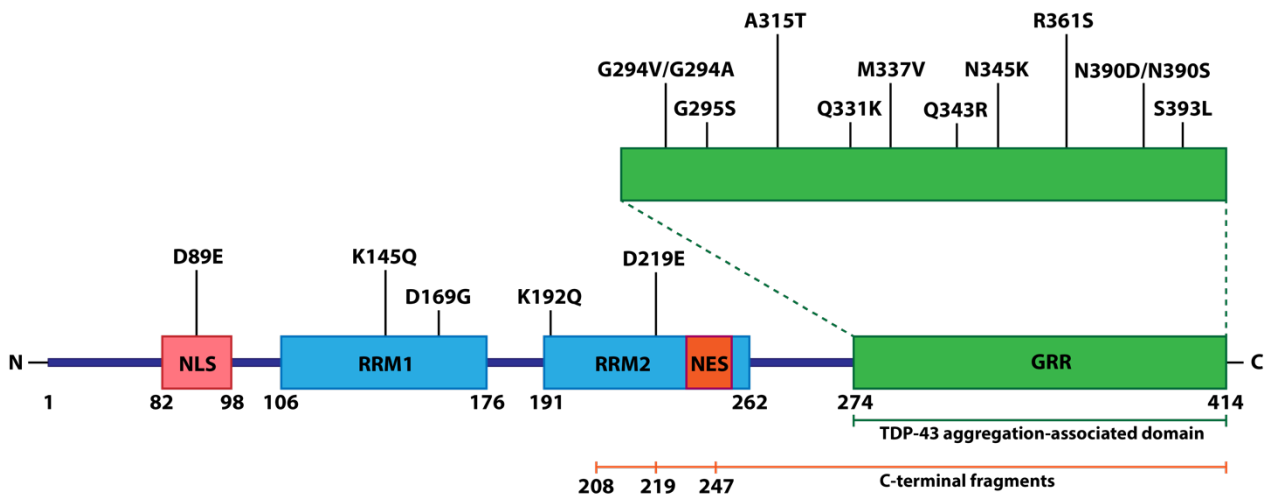

Fig. 1: TDP-43 domain structure and mutations

Schematic illustrating the relevant domains of the TDP-43 protein. It consists of a nuclear localization signal (NLS), two RNA recognition motifs (RRM1 and RRM2) with a nuclear export signal (NES) and a glycine-rich C-terminal region (GRR). Most mutations occur in the GRR. This graph is adapted from Jo et al. (2020) and Cohen et al. (2011).

1.2.1 Isoforms and variants of TDP-43 protein

In the context of neurodegeneration, TDP-43 protein exists in multiple different pathological species. On the one hand, these include shortened and fragmented forms in which the N-terminus becomes truncated, resulting in so-called C-terminal fragments (CTFs). On the other hand, numerous other posttranslational modifications (PTMs) can alter the full-length variant, leading to an ubiquitinated, phosphorylated, SUMOylated or acetylated

molecule prone for misfolding and aggregation (Berning and Walker, 2019). Lastly, a plethora of different mutations in the *TARDBP* gene exist, which account for up to 5 % of familial ALS cases (Ghasemi and Brown, 2018; Giannini et al., 2020). Early on, after the discovery of TDP-43 in neuronal inclusions, it became clear, that differently modified forms of TDP-43 are not evenly distributed throughout the CNS (Igaz et al., 2008). Most notably it was shown that CTFs are predominantly located in cortical and hippocampal areas, while motor neurons incorporate mainly full-length TDP-43 (Igaz et al., 2008). As motor neuron degeneration is the main feature in ALS pathology, it is not surprising that numerous studies have shown that overexpression of full-length TDP-43 in mice can cause both a motor phenotype reminiscent of ALS and is highly toxic to neuronal cells regardless of whether the protein is aggregated or diffusely solubilized (Hergesheimer et al., 2019; Sasaguri et al., 2016; Walker et al., 2015). For TDP-43, the pathological effects of full-length TDP-43 are additionally facilitated by the fact that PTMs can have an influence on aggregation propensity, protein functionality and distribution pattern, especially since many of them occur in the C-terminal region of the protein (Buratti, 2015; Prasad et al., 2019). On top of that, the presence of PTMs is closely linked to cellular stress creating unbalanced elevated levels of reactive oxygen species or reactive nitrogen species which leads to a detrimental situation where prevalence and impact of both PTMs and cellular stress conditions mutually influence and provoke each other (Barber and Shaw, 2010; Li et al., 2013; Niedzielska et al., 2016).

Of special relevance for the present work, PTMs and fragmentation of full-length TDP-43 are not the only relevant aspects affecting its toxicity. A pivotal factor in many neurodegenerative diseases is the aggregation state of the relevant peptides (Chen et al., 2017; Ingelsson, 2016). Typically, the basis of protein aggregation is formed by monomers, whose aggregation continues via oligomers and protofibrils ultimately leading to the formation of protein fibrils. In AD and PD, neurotoxic properties for the distinct aggregates of Amyloid-β (A-β) and α-synuclein vary significantly, revealing an inflammatory response especially towards oligomeric and protofibrillary forms (Alam et al., 2019; Lučiūnaitė et al., 2020). For TDP-43 however, a comparable characterization has so far not been made. Yet this is of eminent importance, not only to determine the toxic properties of full-length

TDP-43 protein in more detail, but also to gain a deeper understanding of its toxicity in the context of an increasingly recognized pathological mechanism called neuroinflammation.

1.3 Neuroinflammation

A critical characteristic of nearly all neurodegenerative disorders is neuroinflammation (Guzman-Martinez et al., 2019). This is defined as an inflammatory response of the central nervous system (CNS). Here, an overactivation of resident immune cells can harm surrounding tissue and result in a vicious cycle of dying neurons which again account for an increased inflammatory response. In recent years it became increasingly eminent that this process plays a key role not only in ALS pathology, but also other neurodegenerative diseases like Alzheimer's or Parkinson's disease and frontotemporal dementia (Heneka et al., 2014; Holbrook et al., 2021).

1.3.1 Microglia in neuroinflammation

Being the primary myeloid cell type of CNS parenchyma, microglial cells are widely implicated in this self-amplifying mechanism of dying neurons and acute inflammation. As part of the innate immune system, microglia possess several classes of receptors, which enable them to sense and respond to their environment. These receptors can recognize certain patterns of binding molecules and are therefore also called pattern recognition receptors (PRRs) (Li and Wu, 2021). As an appropriate response to the respective stimuli has to account for endogenous as well as exogenous signals, these receptors are classified into membrane-bound and cytoplasmic PRRs depending on their cellular localization. Again, these can be divided into five well-defined families, one of them being Toll-like receptors (TLRs) as membrane-bound PRRs, thus playing a key role in the detection of stress signals by innate immune cells (Feldman et al., 2015; Olson and Miller, 2004). A broad variety of receptors belong to this group and the specificity of recognizing different ligands varies between subtypes (Vidya et al., 2018). Of all ten TLRs that have so far been identified in humans, TLR 4 was discovered first and, together with TLR 2, is particularly efficient (Fitzgerald and Kagan, 2020; Sameer and Nissar, 2021). While TLR 4 is activated

especially by microbial lipopolysaccharide (LPS), TLR 2 binds to lipopeptides and pepti-doglycans (de Oliviera Nascimento et al., 2012; Lu et al., 2008). In addition, many TLR subtypes form heterodimers with one another, which increases ligand versatility (Yu et al., 2010). As the basic tripartite structure of PRRs includes an effector domain, they are widely implicated in the initiation of signaling cascades (Li and Wu, 2021). One of the most important ones downstream of these receptors is NF-κB-dependent and leads to the assembly of multimeric intracellular protein complexes referred to as inflammasomes (Boaru et al., 2015). As central signaling hubs for inflammation they are not only capable of a potent reaction towards exogenous microbial molecules called pathogen-associated molecular patterns (PAMPs), but also involved in sensing altered or non-physiological host molecules, known as damage-associated molecular patterns (DAMPs) (Strowig et al., 2012).

1.3.2 NLRP3 Inflammasome

Inflammasomes are multimeric complexes with pivotal functions for the inflammatory response of immune cells (Kelley et al., 2019). Various types of inflammasomes exist, with NOD-, LRR- and pyrin domain-containing 3 (NLRP3) inflammasome being the key immune sensor for danger signals (Heneka et al., 2018). It consists of three essential components: a sensor, an adaptor as well as an effector molecule. All of these components contain different domains enabling them to interact with each other and regulate their activation. The activation of the NLRP3 inflammasome generally requires both steps, priming and activation (McKee and Coll, 2020). The priming step is highly complex and initiates after the binding of PAMPs or DAMPs to specific receptors on the cell membrane that belong to the group of PRRs (Blevins et al., 2022). Consequently, a variety of intracellular signaling cascades are initiated leading to an augmented production of NLRP3 inflammasomal components and pro-inflammatory cytokines like pro-IL-1β and pro-IL-18 (Liu et al., 2017). Upon binding of an adequate stimulus, the NLRP3 inflammasome is activated in a second step, where the previously formed components oligomerize and the pro-inflammatory cytokines are cleaved into their active forms (Voet et al., 2019).

NLRP3 inflammasome activity is tightly controlled. The sensor molecule NLRP3 is a tri-partite molecule which consists of an N-terminal pyrin domain (PYD), a central NACHT domain (acronym of several NACHT-containing proteins) and a leucine-rich repeat do-main (LRR) at its C-terminal end (Swanson et al., 2019). While the NACHT domain is important for NLRP3 oligomerization due to its ATPase activity, the role of LRR is contro-versial as it is linked to both NLRP3 autoinhibition and activation (Duncan et al., 2007; Kelley et al., 2019; Niu et al., 2021). The PYD domain on the other hand serves as a recruiter for the bipartite adaptor protein ASC (apoptosis-associated speck-like protein containing a CARD) by homotypic PYD-PYD interaction, as ASC in turn contains two units: PYD and CARD (caspase recruitment domain) (Lu et al., 2014). This interaction nucleates the filamentous assembly of further ASC molecules into elongated helical struc-tures which then condensate into very large macromolecules referred to as ASC specks (Hochheiser et al., 2022; Sborgi et al., 2015). ASC specks can reach a size of over one micrometer and are the basis for CARD-based and proximity induced autocatalysis of pro-caspase-1 as the final effector molecule of the NLRP3 inflammasome (Heneka et al., 2018; Masumoto et al., 1999). This interaction finally results in a catalytically active heter-otetramer of cleaved caspase-1 p10 and p20 subunits which are particularly capable of processing pro-inflammatory cytokines of the IL-1β family (Sborgi et al., 2015). The de-scribed process of ASC speck formation and inflammasome activation can trigger a feed-forward cascade effect culminating in pyroptosis, a caspase-1 dependent pathway that alters ion fluxes and ultimately results in cell lysis (Bergsbaken et al., 2009). Moreover, it is one of the key mechanisms that account for ongoing inflammation in many devastating neurodegenerative diseases including ALS, AD and PD (Kwon and Koh, 2020). Recent studies have shown that TDP-43 protein can act as a stimulus to initiate this process, reflecting its substantial role in ALS pathology (Deora et al., 2020; Zhao et al., 2015). Given the prevalence of TDP-43-positive inclusions in the vast majority of ALS cases, the connection between TDP-43 and NLRP3 inflammasome-based neuroinflammation is of exceptional importance and at the center of this doctoral thesis.
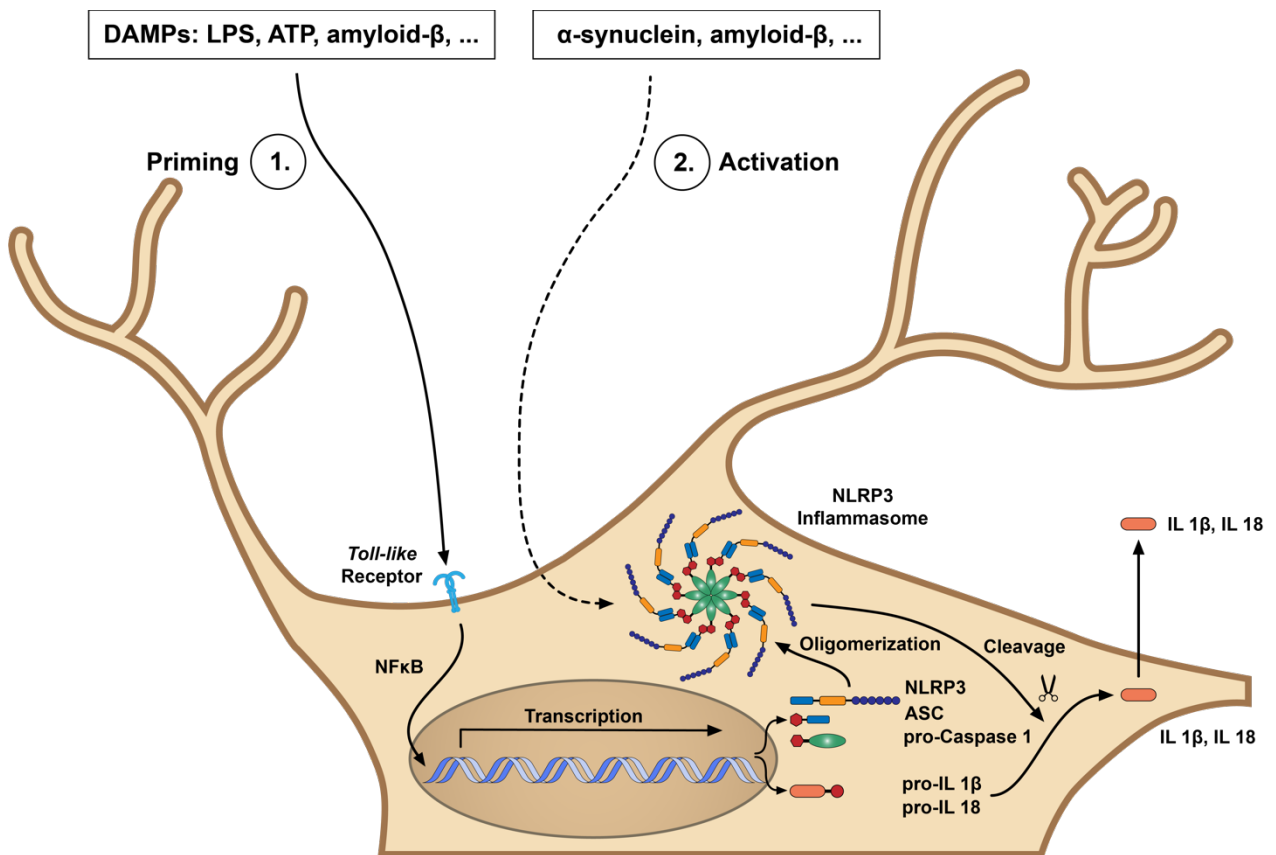
Fig. 2: NLRP3 inflammasome activation in microglial cells

Activation of the NLRP3 inflammasome requires two steps: priming and activation. First, NLRP3 inflammasome components are upregulated via a NF-κB-dependent pathway upon binding of DAMPs to TLRs on the cell surface. Second, after exposure to an adequate stimulus, NLRP3 inflammasome components oligomerize and become activated. Finally, this leads to maturation of IL-1β and IL-18 to their active forms and release into the interstitium.

1.3.3 Experimental models of the NLRP3 inflammasome

For several neurodegenerative diseases a variety of scientific models exist to analyze neuroinflammation (Peng et al., 2021). In this context, the possible involvement of the NLRP3 inflammasome is particularly important, as it is one of its central players. While *in vivo* models are often limited by high costs, restricted availability and ethical constraints alternative sources are essential to study signaling pathways or mechanisms. Therefore, certain cell lines have proven to be particularly suitable for the study of the NLRP3 inflammasome. These include the murine macrophage cell lines RAW264 and J774, as well as

the human monocyte/macrophage cell line THP-1 (Zito et al., 2020). Of note, both murine cell lines differ in a very important aspect. While RAW264 cells are not able to produce ASC, J774 macrophages can (Hirano et al., 2017). On the other hand, THP-1 cells are originally derived from an acute monocytic leukemia patient which leads to genomic instability and a lack of several signaling cascades (Zito et al., 2020). Due to these aspects, but also because of their robust nature, murine J774 cells are often favored for studies of NLRP3 inflammasome stimulation and inhibition (Chang et al., 2015; Di et al., 2018; Marchetti et al., 2018). In addition to cell lines, primary microglial cells are one step closer to the live organism and offer the possibility to strictly control *ante-mortem* conditions, as they form a homogenous genetic population which is specific-pathogen free (Timmerman et al., 2018). This makes them the most widely used *in vitro* modality for microglial studies (Sabogal-Guáqueta et al., 2020).

Regardless of the cell model used, screening studies represent the first step to investigate the NLRP3 inflammasome. For this purpose, the analysis of downstream effectors of inflammasomal activation such as IL-1β is suitable (Nizami et al., 2021). This can be combined with the use of specific NLRP3 inflammasome inhibitors such as CRID3, whose effect is directly visible and can thus consolidate NLRP3 inflammasome involvement. Concerning experimental NLRP3 inflammasome activation itself, standard protocols typically proceed in two steps: priming and activation. Prototypically, this is done by sequential treatment with LPS and nigericin (Zito et al., 2020). Here, LPS causes priming, while nigericin acts as a potassium ionophore, leading to K^+ efflux and thus NLRP3 inflammasome activation (Muñoz-Planillo et al., 2013). Besides the classical sequence of priming and activation, current studies also reveal canonical NLRP3 inflammasome activation in the absence of priming (de Carvalho et al., 2019; Gritsenko et al., 2020). In this regard, an important finding was recently published relating to PD, where data showed that distinct α-synuclein forms were able to do both priming and activation of the NLRP3 inflammasome (Scheiblich et al., 2021). In the context of TDP-43 dependent NLRP3 inflammasome activation, it is intriguing to speculate if the sole exposure of TDP-43 protein is also sufficient not only to prime but also to activate the NLRP3 inflammasome.

1.4 Aims of the study and research question

Taken together, TDP-43 protein plays a pivotal role in many neurodegenerative diseases and is one of the hallmarks of ALS pathology. This is true for both its fragmented forms and especially for the much more widely prevalent wild-type full-length variant. Here, I aimed to elucidate the neuroinflammatory potential of this unaltered TDP-43 isoform and formulated my hypothesis that TDP-43 can act as a DAMP and activates the NLRP3 inflammasome, a multimeric complex of key importance for neuroinflammation.
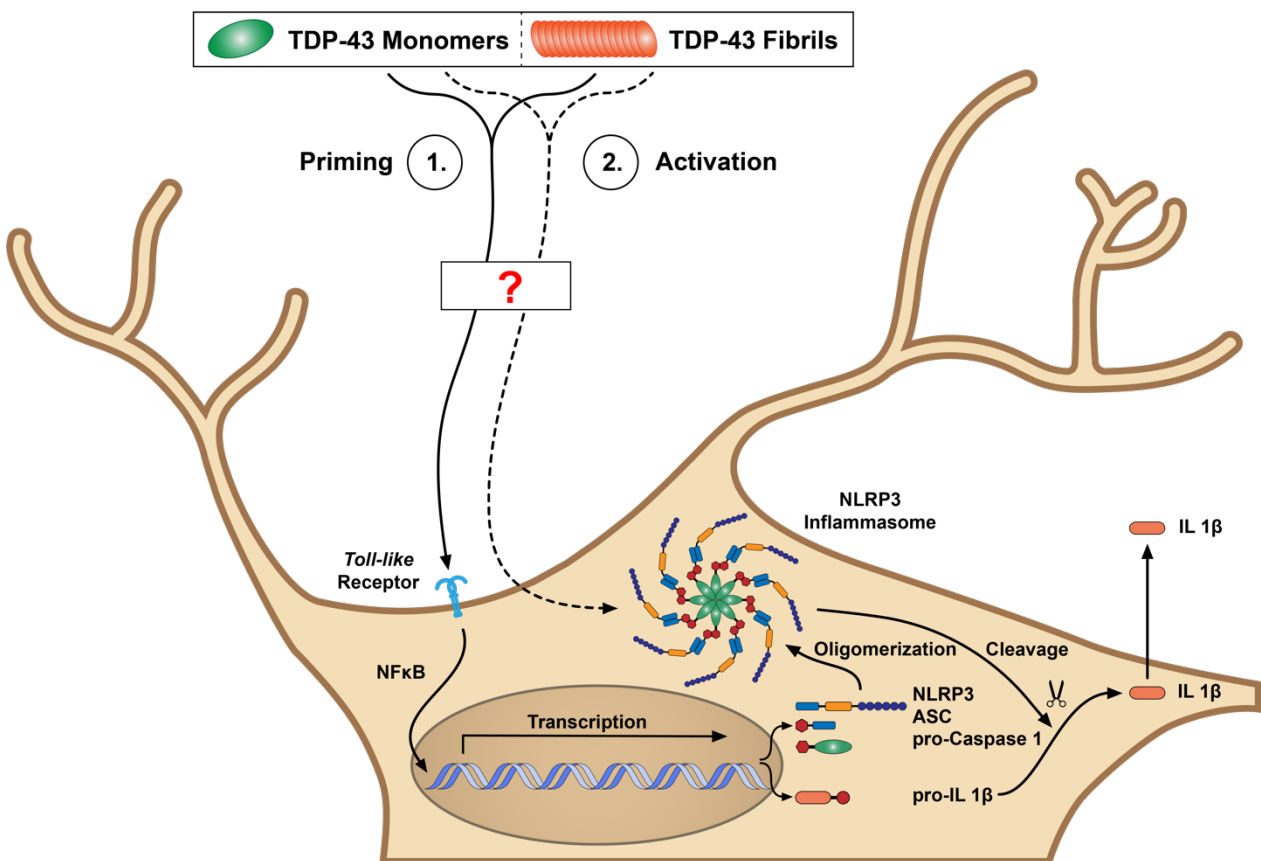

Fig. 3: Involvement of TDP-43 protein species in neuroinflammation

Schematic showing the proposed signaling cascade after exposure of microglial cells to TDP-43 protein species. The key question of this work is whether full-length TDP-43 variants can activate microglia and, if so, whether this occurs in a NLRP3 inflammasome-dependent manner. Besides the involvement of the NLRP3 inflammasome, the role of Toll-like receptors is of special interest.

As the full-length variant of TDP-43 is intrinsically aggregation-prone, possible differences between monomers and fibrils were determined. This discrimination is of major importance, as the neurotoxicity of TDP-43 aggregation is still not described in sufficient detail (Hergesheimer et al., 2019). To test my hypothesis, I followed a three-step approach and conducted experiments using cell lines and primary microglia. These functional experiments were supplemented by structural studies of human origin. To conclude with, I aimed to examine other contributing signaling pathways, including TLRs as central players in stimulatory processes of immune cells.

2. Material and methods

2.1 Animals

All mice used for this study were bred on a C57BL/6 genetic background. The treatment and breeding of animals were in accordance with the German Animal Welfare Act and was approved by the local ethics committee. For this study wild-type mice of mixed gender were used and housed with continuous access to food and water at a temperature of 22 °C in a 12 h light-dark cycle. Performed procedures met the requirements of the state agency for nature, environment and consumer protection of North Rhine-Westphalia (LANUV).

2.2 Cell culture

Experiments were performed using either J774.2 macrophages, a murine monocytic cell line originally derived from BALB/c mice, or primary microglia isolated from postnatal C57BL/6 mice.

J774.2 macrophages were cultured under standard conditions in Dulbecco's modified Eagle's medium (DMEM) complemented with 10 % heat-inactivated Fetal Bovine Serum (iFBS) and 1 % Penicillin/Streptomycin (P/S).

Primary microglia were isolated as described by Giulian and Baker (1986). In brief, brains were collected from male and female mouse pups at postnatal day 0-2 and were carefully stripped off their meninges. Tissue was dissociated by gentle trypsinization and the resulting homogenous cell suspension consisting of mixed glial cells was seeded into poly-L-lysine coated T75 culture flasks (1-2 brains per flask) and left overnight to adhere. At the next day cells were washed with Dulbecco's Phosphate Buffered Saline (DPBS) to remove remaining cell debris and cultured for another 7-10 days in DMEM supplemented with 10 % iFBS, 1 % P/S and 1 % L-929 cell supernatant to provide growth factors. By the end of the cultivation period loosely attached microglial cells were softly shaken off the confluent astrocytic monolayer and used for the respective experiments.

Preceding all experiments, primary microglia or J774.2 macrophages respectively were seeded into well plates using DMEM containing 1 % of serum-free N-2 supplement and left overnight to adhere.

2.3 Human tissue samples

Post-mortem brain sections of two TDP-43 positive sporadic ALS patients were provided by the DZNE Brain Bank Bonn. Paraffin-embedded brain material from three different neuronal areas (precentral gyrus, cerebellum and ventral horn of the spinal cord) was sliced using a microtome into sections with a thickness of 5 μm. For analysis, relevant ethical regulations were followed and all patients consented to the use of their brain material for medical research.

2.4 TDP-43 protein samples

The proteins used for the experiments were kindly provided by our collaborators from the Lashuel Laboratory at EFPL in Lausanne, Switzerland. Proteins were aliquoted at a concentration of 3.3 μM (monomers) or 4.5 μM (fibrils) and solubilized in a Tris-buffer of 50 mM Tris, 200 mM NaCl and 1 mM DTT at pH 7.4. Monomers were stored at a temperature of -80 °C, fibrils at 4 °C.

2.5 Electron microscopy

For morphological identification of protein samples negative staining electron microscopy was used. Preparation of TDP-43 samples and acquisition of pictures was performed in collaboration with the AG Geyer from the Institute of Structural Biology Biomedical Center (BMZ) in Bonn. Protein solutions were applied onto a glow discharged copper grid and incubated for one minute. After a following washing step, samples were negatively stained with a dilute electron-opaque solution of 2 % uranyl acetate for 30 seconds. Remaining

fluids were removed and grids were air-dried. Immediately, imaging of samples was performed with a JEOL JEM-2200FS 200 kV Transmission Electron Microscope (TEM) using a CMOS-based Camera.

2.6 Measurement of cytokine secretion

As a marker for NLRP3 inflammasome activation by monomeric and fibrillary TDP-43 protein, the concentration of secreted IL-1β into cell supernatants was measured using the Mouse IL-1 beta/IL-1F2 DuoSet ELISA Kit. For the generation of samples, cells were plated at a density of 7.5 x 10^4 cells/well in 96-well plates or 2 x 10^6 cells/well in 6-well plates, left overnight to attach and then treated with the stimuli to be tested or under control conditions. To inhibit the NLRP3 inflammasome specifically, cells were incubated with Cytokine Release Inhibitory Drug 3 (CRID3; also known as MCC950), or IFM-2384 30 min before and during the treatment both at a concentration of 1 µM. Thereafter, cell supernatants were collected and assayed according to manufacturer's protocol. Briefly, microplates were coated with a capture antibody for IL-1β and left overnight to adhere. At the next day plates were blocked and then incubated with the pre-generated protein samples or standards respectively. Subsequently the detection antibody was added and further incubation steps with Streptavidin-HRP and substrate solution followed. The reaction was stopped by addition of a stop solution and optical density was measured using a microplate reader. To quantify the respective concentrations of the samples, a standard curve was used for interpolation.

For experiments with Toll-like receptor inhibition, anti-mouse TLR2 antibody, anti-mouse TLR5 antibody and anti-mouse TLR4/MD-2 Complex antibody were used. Each of them was co-incubated at a concentration of 5 µg/mL with the respective stimulatory agents.

For quantification of a broad spectrum of cytokine secretion by primary microglia the Proteome Profile Mouse Cytokine Array Panel A was used, able to simultaneously detect 40 cytokines, chemokines and acute phase proteins. Supernatant of primary microglial cells was analyzed as per manufacturer's protocol. Briefly, the kit's membranes were blocked and then incubated overnight with the respective samples, array buffers as well as an

antibody cocktail. After three washing steps membranes were incubated with IRDye$^{®}$ 800CW Streptavidin (1:20.000) for 30 min and subsequently imaged. Images were taken with an Odyssey$^{®}$ CLx Imaging System, followed by data analysis with Image Studio software.

2.7 Cell viability and Cytotoxicity assays

To assess cell viability either the XTT Cell Viability Kit or the MTT Cell Proliferation Kit I were used according to manufacturer's protocols. Briefly, primary microglia or murine J774.2 cells were plated with a density of 7.5 x 10^4 cells/well in 96-well plates and left overnight to adhere. After treatment with various stimuli either an XTT or MTT assay was performed. For the XTT assay DMEM was mixed with an XTT reagent and an Electron Coupling Solution and added to the cells, whereas for the MTT assay an MTT labeling reagent and a solubilization solution were added successively. Incubation times complied with the respective protocols. Absorbance was measured at 450 nm (XTT) or 630 nm (MTT) using a microplate reader, with acquired results reflecting the metabolic activity of the treated cells.

Cellular cytotoxicity was determined with the Cytotoxicity Detection Kit (LDH) as LDH release into cell supernatants is proportional with a damaged plasma membrane. Following the manufacturer's protocol, a reaction mixture of Dye Solution and a Catalyst were added to 50 µl of respective supernatants. Afterwards the concentration of LDH was photometrically quantified at 490 nm with a microplate reader.

2.8 Western Blot

J774.2 macrophages or primary microglia were seeded (2 x 10^6 cells/well in 6-well plates or 1 x 10^6 cells/well in 12-well plates) and stimulated either under control conditions or with the stimuli to be tested. Following the respective simulation periods, cell supernatant was collected and the remaining cells were lysed on ice with radioimmunoprecipitation assay (RIPA) lysis buffer (50 mM Tris-HCl, 1 % Triton X-100, 0.5 % sodium deoxycholate,

0.1 % sodium dodecyl sulfate (SDS), 150 mM NaCl, pH 7.2) containing 1X phosphatase inhibitor cocktail.

In order to yield a sufficient protein concentration in cell supernatants, samples were precipitated using chloroform-methanol precipitation as described by Scheiblich et al. (2017). In brief, 500 µl of ice-cold methanol and 125 µl chloroform were added to 500 µl of cell supernatant. Samples were then vortexed and centrifuged vigorously at 13.000 x g for five minutes, obtaining two separate phases of which the upper phase was discharged. Once again 500 µl methanol were added and samples were vortexed and centrifugated (13.000 x g, 5 min). The supernatant was cautiously removed and the remaining protein pellet was dried for five minutes in a vacuum concentrator at 45 °C. The dried pellet was then resuspended in 2X Loading Buffer and denatured for five minutes at 95 °C, after which the samples were ready for Western Blot analysis.

Cell lysates and precipitated supernatant samples were separated using a NuPAGE® 4–12 % Bis-Tris Gel and then transferred onto nitrocellulose membranes. These membranes were blocked with 3 % BSA in Tris-buffered saline supplemented with Tween-20 (TBST; 10 mM Tris-HCl, 150 mM NaCl, 0.05 % Tween-20, pH 8.0) for one hour and subsequently incubated overnight with the following antibodies against components of the NLRP3 inflammasome: rat anti-caspase-1, rabbit anti-ASC, mouse anti-NLRP3 and mouse anti-α-tubulin. All antibodies used were diluted 1:1000 in blocking solution (3 % BSA in TBST). Detection of primary antibodies was performed with IRDye® 680RD goat anti-rabbit IgG, IRDye® 800CW goat anti-rat IgG and IRDye® 680RD goat anti-mouse IgG in a dilution of 1:20.000. For visualization of secondary antibodies, an Odyssey® CLx Imaging System was used, followed by data analysis with Image Studio software.

2.9 FLICA assay

To detect active Caspase-1 as the main effector of NLRP3 inflammasome activation, the FAM-FLICA Caspase-1 Assay (FLICA = Fluorochrome-Labeled Inhibitors of Caspases) was used according to manufacturer's protocol. Briefly, FAM-FLICA inhibitor reagent (FAM-YVAD-FMK) was added to the supernatant of treated cells and incubated for one hour. Ten minutes before the end of the incubation period 0.5 % of Propidium Iodide (PI)

was added. Three washing steps of ten minutes each with Apoptosis Wash Buffer followed to allow the diffusion of unbound FLICA reagent out of the cells. Thereafter, cells were trypsinized (0.25 %) for ten minutes, washed again and then collected. After generation of the respective compensation controls, the samples were analyzed using a BD FACSCanto™ II Flow Cytometer. For detailed analysis and quantification FlowJo software was used.

2.10 Immunohistochemistry

Paraffin slices were deparaffinated and rehydrated using consecutive washing steps in xylene and decreasing concentrations of ethanol and were finally placed in distilled water. For antigen retrieval rehydrated tissue was boiled for ten minutes in 10 mM sodium citrate buffer (pH 6.0) and subsequently allowed to cool down at room temperature for 30 minutes. Following three washing steps in distilled water, sections were incubated for ten minutes with 3 % hydrogen peroxide at 4 °C to block endogenous peroxide activity. After another two washing steps in distilled water and five minutes in PBST (0.1 % Triton), slices were blocked with 5 % normal donkey serum (NDS) in PBST for one hour. Blocking buffer was removed, replaced with primary antibodies solution and incubated overnight at 4 °C. Primary antibodies used were rat anti-TDP-43 as well as goat anti-AIF-1/Iba-1 and were diluted in blocking buffer 1:300 (anti-TDP-43) or 1:500 (Iba-1). Following three washing steps of five minutes each in PBST, sections were incubated with the secondary antibodies donkey anti-rat-Alexa Fluor 488 and donkey anti-goat-Alexa Fluor 555 (both 1:250) for two hours. The tissue was nuclear counter-stained with DAPI (0.1 mg/mL). For imaging of stained sections, a Zeiss LSM 800 microscope was used. Processing and analyzation of taken images was done using Fiji ImageJ software. 3D reconstruction of taken images was performed with Imaris - Microscope Image Analysis Software.

2.11 Statistical analysis

Statistical analysis was performed using GraphPad Prism software version 9. In all graphs data is presented as mean ± standard errors of the mean (SEM) of at least three independent experiments with up to three replicates and is analyzed for a Gaussian distribution. When normality tests were passed, a one-way analysis of variance (ANOVA) followed by Tukey's post hoc test was used to compare between control and treatment groups. If a Gaussian distribution was not followed, data were analyzed as non-parametric with the Kruskal-Wallis test and Dunn's post hoc test. P-values were considered statistically significant below a value of 0.05. Significance levels are indicated as $*p < 0.05$; $**p < 0.01$; $***p < 0.001$ and $****p < 0.0001$. Specific statistical procedures used are mentioned in the figure legends.

2.12 Resources

Tab. 1: Antibodies

Antibodies	Source	Identifier
alpha Tubulin Monoclonal Antibody (DM1A)	Thermo Fisher Scientific, Waltham, MA, USA	Cat# 62204, RRID:AB_1965960
anti-Asc pAb (AL177) antibody	Adipogen, San Diego, CA, USA	Cat# AG-25B-0006, RRID:AB_2490440
Anti-mTLR5-IgG, 100 µg antibody	Invivogen, San Diego, CA, USA	Cat# mabg-mtlr5, RRID:AB_11124926
anti-NLRP3/NALP3 mAb (Cryo-2) antibody	Adipogen, San Diego, CA, USA	Cat# AG-20B-0014, RRID:AB_2490202
Donkey anti-Goat IgG (H+L), Alexa Fluor™ Plus 555	Thermo Fisher Scientific, Waltham, MA, USA	Cat# A32816, RRID:AB_2762839
Donkey anti-Rat IgG (H+L), Alexa Fluor™ 488	Thermo Fisher Scientific, Waltham, MA, USA	Cat# A-21208, RRID:AB_2535794

FITC anti-mouse IgG1 antibody	Biolegend, San Diego, CA, USA	Cat# 406605, RRID:AB_493292
Iba1 Antibody	Novus Biologicals, Littleton, CO, USA	Cat# NB 100-1028, RRID:AB_521594
IRDye® 680RD Goat anti-Mouse IgG antibody	LI-COR Biosciences, Lincoln, NE, USA	Cat# 926-68070, RRID:AB_10956588
IRDye® 680RD Goat anti-Rabbit IgG antibody	LI-COR Biosciences, Lincoln, NE, USA	Cat# 926-68071, RRID:AB_10956166
IRDye® 800CW Goat anti-Rat IgG antibody	LI-COR Biosciences, Lincoln, NE, USA	Cat# 926-32219, RRID:AB_1850025
MAb-mTLR2, 100 µg antibody	Invivogen, San Diego, CA, USA	Cat# mab-mtlr2, RRID:AB_763722
PE anti-mouse IgG1 antibody	Biolegend, San Diego, CA, USA	Cat# 406607, RRID:AB_10551439
Purified (azide-free) anti-TDP43 antibody	Biolegend, San Diego, CA, USA	Cat# 808301, RRID:AB_2564740
Rat anti-Caspase-1 (clone 4B4) antibody	Genentech, South San Francisco, CA, USA	Cat# CASP-1(mu):4175
TLR4/MD-2 Complex Monoclonal Antibody (MTS510)	Thermo Fisher Scientific, Waltham, MA, USA	Cat# MA5-16210, RRID:AB_2537728

Tab. 2: Biological samples and experimental models

Material	Source	Identifier
C57BL/6 mice	Charles River Laboratories, Wilmington, MA, USA	RRID: IMSR_JAX:000664
Human *post-mortem* brain sections	DZNE Brain Bank Bonn	N/A
J774.2 Cell Line from mouse	Sigma-Aldrich, St. Louis, MIS, USA	Cat# 85011428
NCTC clone 929 (L929 cells), strain: C3H/An	ATCC, Manassas, VA, USA	Cat# CCL-1, RRID:CVCL_0462

Tab. 3: Chemicals and peptides

Reagents and Resources	Source	Identifier
1-Step™ Ultra TMB-ELISA Substrate Solution	Thermo Fisher Scientific, Waltham, MA, USA	Cat# 34028
4',6-Diamidino-2'-phenylin-dol-dihydrochloride (DAPI)	Thermo Fisher Scientific, Waltham, MA, USA	Cat# 62247
Bovine Serum Albumin - Fraction V	Rockland Immunochemi-cals, Pottstown, PA, USA	Cat# BSA-1000
CRID3 (MCC950)	Invivogen, San Diego, CA, USA	Cat# inh-mcc
Dulbecco's Modified Ea-gle's Medium	Thermo Fisher Scientific, Waltham, MA, USA	Cat# 31966047
Dulbecco's Phosphate-Buffered Saline	Thermo Fisher Scientific, Waltham, MA, USA	Cat# 14190169
Fetal Bovine Serum	Thermo Fisher Scientific, Waltham, MA, USA	Cat# 10270106
IFM-2384	IFM Therapeutics, Boston, MA, USA	N/A
IRDye® 800CW Streptavi-din	LI-COR Biosciences, Lin-coln, NE, USA	Cat# 926-32230
Lipopolysaccharide from *Escherichia coli* K12	Invivogen, San Diego, CA, USA	Cat# tlrl-eklps
N2-Supplement	Thermo Fisher Scientific, Waltham, MA, USA	Cat# 17502048
Nigericin	Invivogen, San Diego, CA, USA	Cat# tlrl-nig
Normal Donkey Serum	Abcam, Cambridge, UK	Cat# ab7475
NuPAGE® MES SDS Run-ning Buffer (20X)	Thermo Fisher Scientific, Waltham, MA, USA	Cat# NP0002
Orange G	Carl Roth, Karlsruhe, Ger-many	Cat# 0318.2

PageRuler™ Plus Pres-tained Protein Ladder, 10 to 250 kDa	Thermo Fisher Scientific, Waltham, MA, USA	Cat# 26619
Penicillin/Streptomycin	Thermo Fisher Scientific, Waltham, MA, USA	Cat# 15070063
Poly-L-lysine hydrobromide	Sigma-Aldrich, St. Louis, MIS, USA	Cat# P1524
Protease/Phosphatase In-hibitor Cocktail	Cell Signaling, Danvers, MA, USA	Cat# 5872
Sodium dodecyl sulfate (SDS)	Carl Roth, Karlsruhe, Ger-many	Cat# CN30.2
TDP-43 Protein	Hilal Lashuel Group, EPFL, Lausanne	N/A
Triton™ X-100	Sigma-Aldrich, St. Louis, MIS, USA	Cat# T8787
Trypan Blue Solution, 0.4 %	Thermo Fisher Scientific, Waltham, MA, USA	Cat# 15250061
Trypsin-EDTA (0.5 %), no phenol red	Thermo Fisher Scientific, Waltham, MA, USA	Cat# 15400054
Tween™ 20 Surfact-Amps™ Detergent	Thermo Fisher Scientific, Waltham, MA, USA	Cat# 85113

Tab. 4: Commercial assays and kits

Assay/Kit	Source	Identifier
Mouse IL-1 beta/IL-1F2 DuoSet ELISA	R&D Systems, Minneapolis, MN, USA	Cat# DY401
Proteome Profiler Mouse Cytokine Array Kit, Panel A	R&D Systems, Minneapolis, MN, USA	Cat# ARY006
Pierce™ BCA Protein Assay Kit	Thermo Fisher Scientific, Waltham, MA, USA	Cat# 23225
XTT Cell Viability Kit	Cell Signaling, Danvers, MA, USA	Cat# 9095
Cell Proliferation Kit I (MTT)	Roche, Basel, Switzerland	Cat# 11465007001
Cytotoxicity Detection Kit (LDH)	Roche, Basel, Switzerland	Cat# 11644793001
FAM-FLICA® Caspase-1 (YVAD) Assay Kit	Immunochemistry Technologies, Davis, CA, USA	Cat# 97

Tab. 5: Expendable material

Material	Source
96-Well ELISA-Microplates	Greiner Bio-One, Kremsmünster, Austria
96-Well Plates for Pierce™ BCA-RAC Assay	Thermo Fisher Scientific, Waltham, MA, USA
CELLSTAR® Cell culture flasks	Greiner Bio-One, Kremsmünster, Austria
CELLSTAR® Cell culture plates	Greiner Bio-One, Kremsmünster, Austria
Eppendorf Tubes®	Eppendorf, Hamburg, Germany
Falcon® Conical Centrifuge Tubes	Corning, Corning, NY, USA
Nitrocellulose Membrane, 0.2 μm	Bio-Rad Laboratories, Hercules, CA, USA
NuPAGE® 4–12 % Bis-Tris gel	Thermo Fisher Scientific, Waltham, MA, USA
Pipette Tips	Sarstedt, Nümbrecht, DE
Stripette™ Serological Pipets	Corning, Corning, NY, USA
Trans-Blot® Turbo Mini Nitrocellulose Transfer Packs	Bio-Rad Laboratories, Hercules, CA, USA

Tab. 6: Laboratory equipment

Resource	Source
BD FACSCanto™ II Flow Cytometer	BD, Franklin Lakes, NJ, USA
Centrifuge 5424 R	Eppendorf, Hamburg, Germany
Centrifuge 5430 R	Eppendorf, Hamburg, Germany
CO_2 incubator ICO240	Memmert, Schwabach, Germany
Consort EV series power supplies	Sigma-Aldrich, St. Louis, MIS, USA
DURAN® borosilicate glass tubing	Schott, Jena, Germany
Eppendorf Easypet® 3	Eppendorf, Hamburg, Germany
Eppendorf Research® plus Pipette	Eppendorf, Hamburg, Germany
Eppendorf ThermoMixer® C	Eppendorf, Hamburg, Germany
Eppendorf® Multipette® M4 pipette	Eppendorf, Hamburg, Germany
Infinite M200 Pro	TECAN, Männedorf, Switerland
JEM-2200FS Field Emission Electron Microscope	Jeol, Tokyo, Japan
MediLine Lab Fridge	Liebherr, Kirchdorf, Germany
Megafuge 40R	Thermo Fisher Scientific, Waltham, MA, USA
ODYSSEY CLx Imaging System	LI-COR Biosciences, Lincoln, NE, USA
Ohaus Adventurer™ Analytical Scale	Ohaus, Parsippany, NJ, USA
Primovert Inverted Microscope	Carl Zeiss, Oberkochen, Germany
Rocking platform shaker, VWR®	Avantor, Radnor, PA, USA
Safe 2020 Class II Biological Safety Cabinet	Thermo Fisher Scientific, Waltham, MA, USA
TemCam-F416 CMOS based Camera	TVIPS, Gauting, Germany
Trans-Blot Turbo Transfer System	Bio-Rad Laboratories, Hercules, CA, USA
Transferpette® S	Brand, Wertheim, Germany
Unimax 1010 Shaker	Heidolph, Schwabach, Germany
V86-500i Freezer	Ewald, Rodenburg, Germany
Vortex-Genie 2	Scientific Industries, Bohemia, NY, USA
Water Bath 1012	GFL, Burgwedel, Germany

XCell4 SureLock™ Midi-Cell	Thermo Fisher Scientific, Waltham, MA, USA
Zeiss Laser Scan Microscope 800	Carl Zeiss, Oberkochen, Germany

Tab. 7: Software and algorithms

Software	Source	Identifier
Adobe Illustrator	Adobe, San José, CA, USA	v27.2
Excel	Microsoft, Richmond, WA, USA	v16.63.1
Fiji ImageJ	Wayne Rusband, National Institute of Health, Bethesda, MD, USA	v2.3.0/1.53q
FlowJo	BD, Franklin Lakes, NJ, USA	v10.8.1
Graph Pad Prism	Graphpad Software Inc., CA, USA	v9.3.1
Image Studio	LI-COR Biosciences, Lincoln, NE, USA	v5.2
Imaris	Oxford Instruments, Abingdon, UK	v9.2.1
NIS-elements	Nikon, Tokyo, Japan	v4.2

3. Results

3.1 Monomeric TDP-43 dose-dependently induces inflammatory response in J774.2 macrophages

In order to test common pathways in the activation of innate immune cells the effect of differently aggregated TDP-43 proteins was investigated on murine J774.2 macrophages *in vitro*. Prior to these experiments, the morphology of proteins under consideration was confirmed by electron microscopy (Figure 4A+B) and Western blot (Figure 4C).
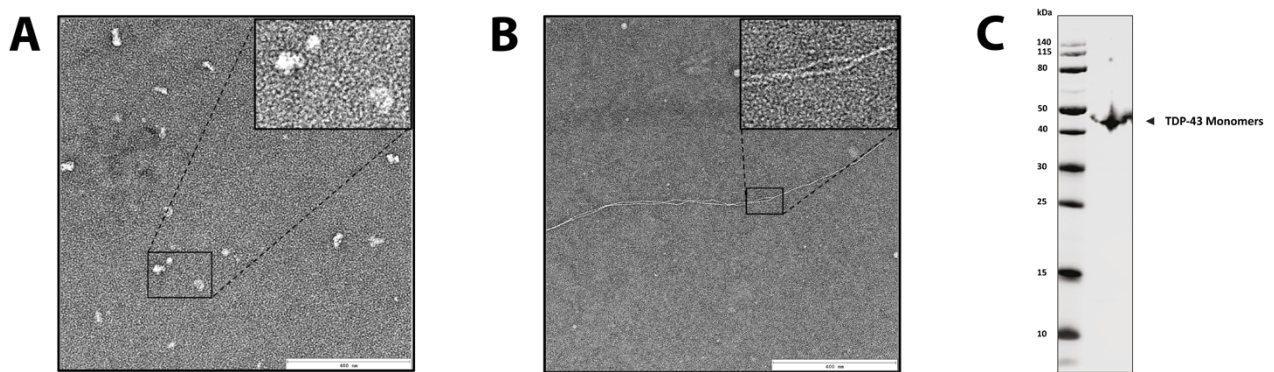
Fig. 4: Examination of TDP-43 morphology

Electron microscopy images of TDP-43 monomers (A) and fibrils (B). Scale bar 400 nm. (C) Western blot analysis of TDP-43 protein stock using TDP-43 specific antibody.

Monomers and fibrils showed their typical appearance of either small protein aggregates or well-defined fibrils, some of which partially bundled, and a strong and clearly visible Western blot band at the eponymous molecular weight of 43 kDa confirmed the presence of TDP-43 protein.

To allow for a standardized experimental approach, a continuous procedure was implemented (Figure 5). For this purpose, J774.2 macrophages were seeded into the well plates prior to each experiment and left overnight to adhere. At the next day a 24-hour stimulation with either TDP-43 monomers or fibrils was performed. The analogous regime was used for the later described experiments with primary microglia (for details, see below).
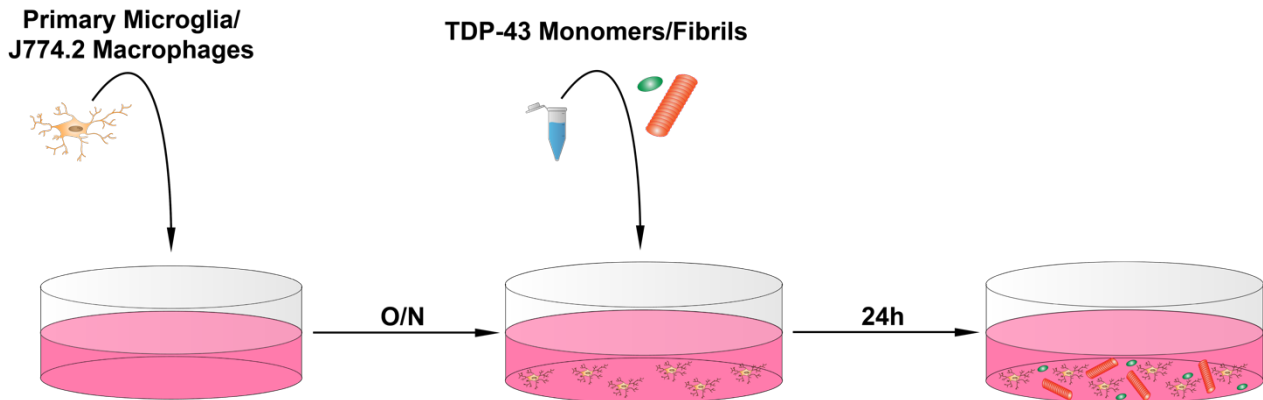
Fig. 5: Methodological Approach

Schematic showing the experimental setup used in this project.

For evaluation of sufficiently stimulating protein concentrations, cells were treated with monomeric or fibrillary TDP-43 forms in rising doses, after which inflammasomal activity was determined in cell supernatants using ELISA-based quantification of IL-1β protein as the main product of NLRP3 inflammasome activation (Figure 6A).
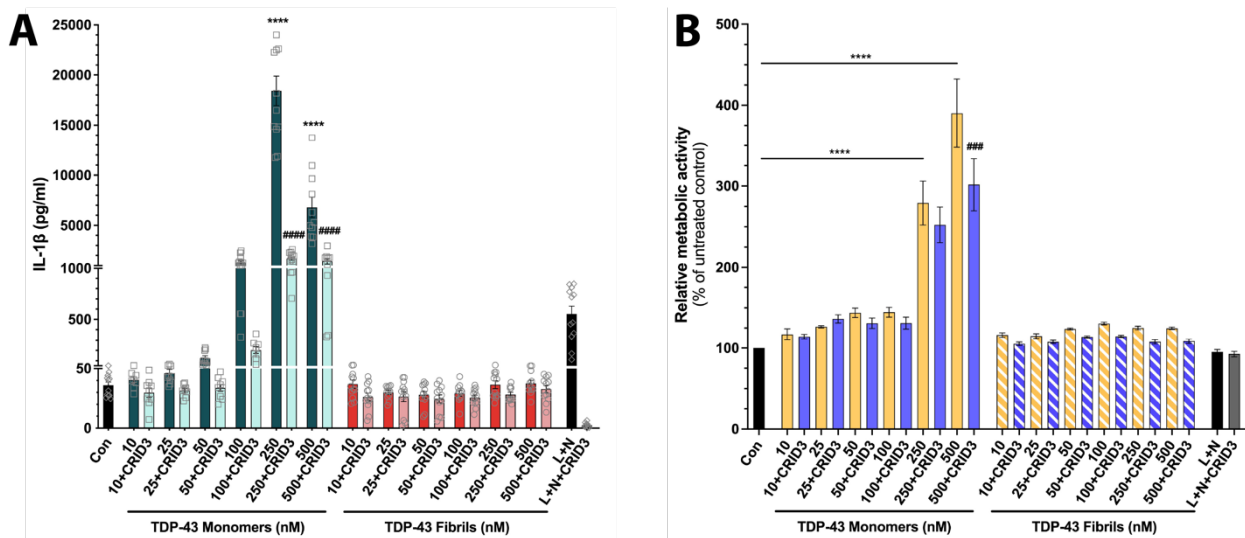

Fig. 6: Dose-response of TDP-43 peptide treatment in J774.2 macrophages

Stimulation of J774.2 cells (7.5 x 10^4 cells/well) with TDP-43 monomers/fibrils (24 h) with or without NLRP3-inflammasome inhibitor (CRID3, 1 µM). LPS (L; 3 h, 100 ng/ml) and Nigericin (N; 1 h, 5 µM) were used as positive control. IL-1β ELISA of supernatant (A) and XTT-assay of stimulated cells (B). Data is shown from four independent experiments (n = 4) with triplicate measurements (N = 12). Graphs are presented as mean ± SEM and analyzed by one-way ANOVA with post hoc Tukey's test. Levels of significance are indicated as *p < 0.05; **p < 0.01; ***p < 0.001 and ****p < 0.0001; ###p < 0.001 and ####p < 0.0001 vs. uninhibited concentration.

Monomeric TDP-43 protein strongly and dose-dependently induced IL-1β secretion, even exceeding the effect of a sequential treatment with LPS and Nigericin. Interestingly, fibrillary TDP-43 was not able to cause a similar effect in this setting.

To further probe the underlying molecular mechanism, stimulated cells were co-treated with the NLRP3 inflammasome inhibitor CRID3 which resulted in significantly diminished levels of IL-1β secretion compared to treatment with sole TDP-43 monomers and unaltered values when TDP-43 fibrils were used (Figure 6A). Subsequently, an XTT assay of the stimulated cells was performed to evaluate metabolic activity. High levels of activation were found when exposed to monomeric TDP-43, whereas TDP-43 fibrils did not alter activity levels compared to the untreated control (Figure 6B). Also, exposure to LPS and Nigericin did not have an influence on metabolic activity.

3.2 NLRP3 inflammasome is part of induced signaling pathways

As the next step, Western blot analysis was used to confirm the involvement of the NLRP3 inflammasome in induced metabolic pathways. Indeed, stimulated cells upregulated the intracellular concentration of NLRP3 protein and cleaved Caspase-1 together with ASC was released into cell supernatants after exposure to monomeric TDP-43 (Figure 7B, E and F). From all NLPR3 inflammasome components only intracellular ASC protein was not significantly upregulated, although some sporadically elevated values were detected (Figure 7C). Most importantly, treated cells were again co-incubated with specific inhibitors of the NLRP3 inflammasome. Besides CRID3, IFM as a second inhibitor of the NLRP3 inflammasome confirmed these results. Similar to IL-1β secretion, both IFM and CRID3 significantly diminished the inflammatory release of NLRP3 inflammasome components into extracellular space. While a significant attenuation on ASC release was reached with both inhibitors, the effect on secretion of cleaved Caspase-1 was more pronounced with IFM. CRID3 on the other hand, missed the threshold of significance (p = 0.26). Of note, concentration of intracellular NLRP3 protein persisted on an elevated level after application of NLRP3 inhibitors. In line with previous findings, when cells were treated with TDP-43 fibrils neither inflammasomal components were upregulated, nor released into the supernatant.
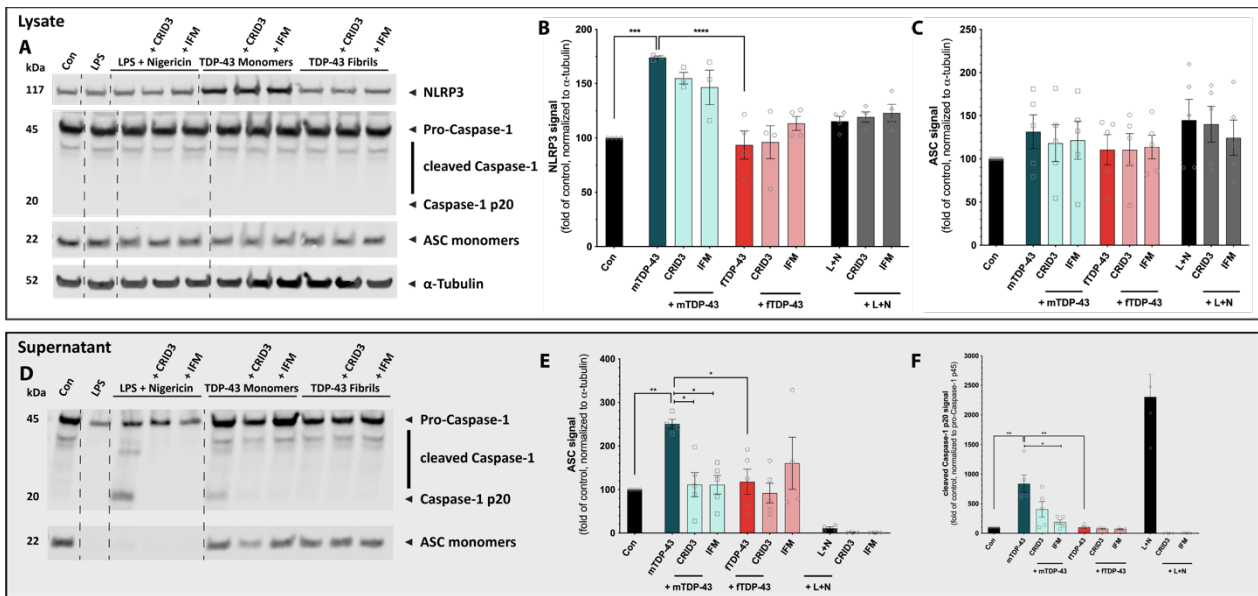
Fig. 7: Induction of NLRP3 inflammasome components by TDP-43 protein in J774.2 macrophages

Western Blot analysis and quantification of stimulated J774.2 cells. Dotted vertical lines indicate spliced sections. Only data used for this project is shown. Quantification of the inflammasomal components NLRP3 (B), ASC (C and E) and cleaved Caspase-1 (F). Cells were seeded at a density of 2×10^6 cells/ well. TDP-43 monomers/ fibrils (mTDP/ fTDP; 100 nM, 24 h) and NLRP3-inflammasome inhibitor (CRID3 or IFM, 1 µM) were used as treatment. LPS (L; 3 h, 100 ng/ml) and Nigericin (N; 1 h, 5 µM) was used as a positive control. Data is shown from five independent experiments (n = 5) and is displayed as mean ± SEM. Analysis of samples is done with one-way ANOVA and post hoc Tukey's test. Levels of significance are indicated as $*p < 0.05$; $**p < 0.01$; $***p < 0.001$ and $****p < 0.0001$.

To probe the involvement of NLRP3 inflammasome more completely, extracellular IL-1β secretion as the main resulting cytokine from inflammasomal activation was quantified using ELISA (Figure 8A). The results were similar to the dose-response experiments, especially the stimulatory potential of monomeric TDP-43, as well as potent inhibition by CRID3 and IFM was confirmed (Figure 8A). In the respective lactate dehydrogenase (LDH) assays no significant difference between TDP-43 stimuli was found when compared to untreated controls (Figure 8B). LDH levels were significantly lowered after successive treatment with LPS and Nigericin, regardless of whether NLRP3 inhibitors were used.
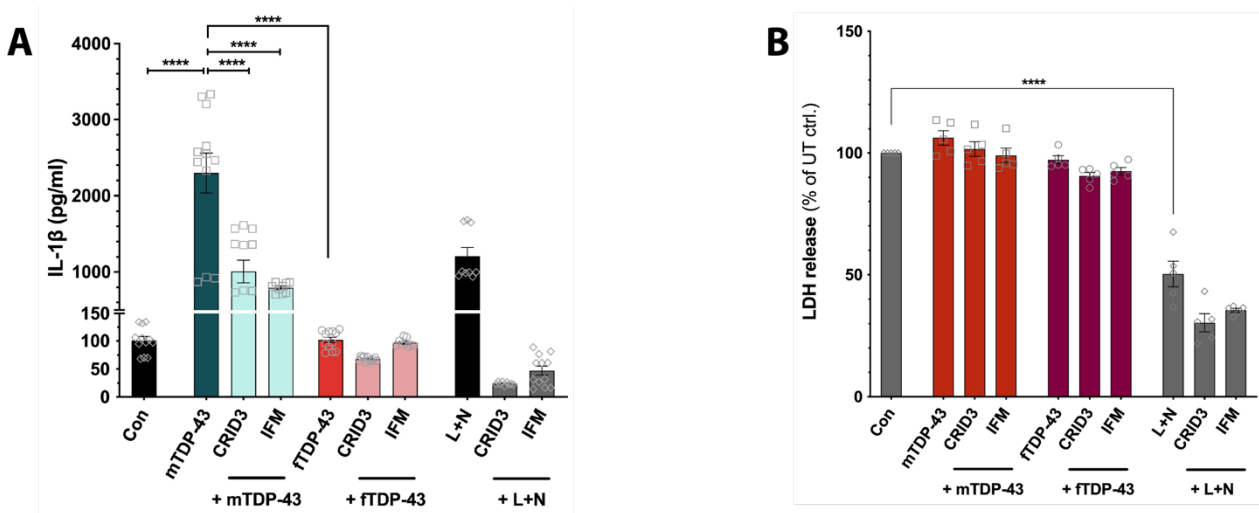
Fig. 8: IL-1β secretion and cytotoxicity after TDP-43 exposure of J774.2 macrophages

(A) IL-1β ELISA of supernatant from Western Blot experiments. (B) LDH assay from cell supernatant. Sample preparation and statistical analysis as in Figure 7.

3.3 Primary microglia also reveal an inflammatory response to TDP-43 protein

To confirm cell-line findings, the next set of experiments was pursued with primary microglia. As expected, a progressively increasing, dose-dependent release of IL-1β was found when cells were subjected with TDP-43 monomers (Figure 9A). Similar to J774.2 macrophages, the stimulatory potential of monomeric TDP-43 clearly exceeded the effect of LPS and Nigericin. Moreover, inhibition of inflammatory effects with both CRID3 and IFM was particularly strong at high peptide concentrations, while in lower doses only IFM diminished the release of cytokines significantly. Surprisingly, stimulation of primary microglia with rising concentrations of fibrillary TDP-43 also lead to an increased secretion of IL-1β. However, values reached were orders of magnitude smaller than the TDP-43 monomers results.

Consistent with J774.2 macrophages, cell viability assays showed high and dose-dependent metabolic activity of microglia in response to TDP-43 monomer stimulation (Figure 9B). Co-incubation with NLRP3 inflammasome inhibitors did not differ from uninhibited peptide treatment.
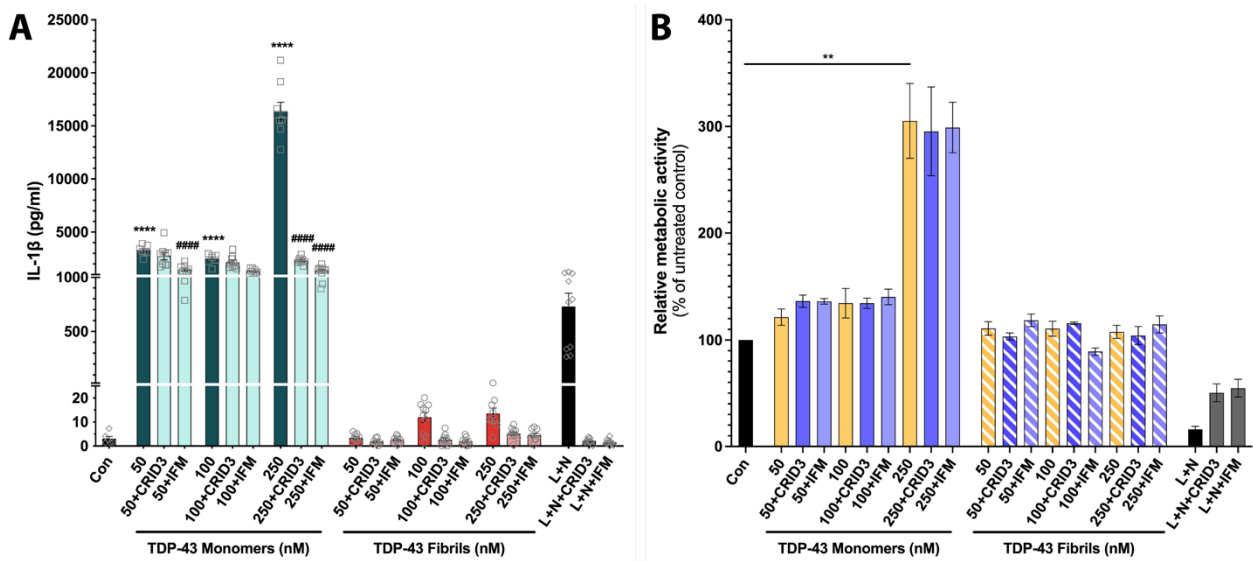
Fig. 9: Dose-response of TDP-43 peptide treatment in primary microglia

Stimulation of primary microglia (7.5×10^4 cells/ well) with TDP-43 monomers/ fibrils (24 h) with or without NLRP3 inflammasome inhibition (CRID3 or IFM, 1 µM). LPS (L; 3 h, 100 ng/ml) and Nigericin (N; 1 h, 5 µM) were used as positive control. IL-1β ELISA of supernatant (A) and MTT-Assay of stimulated cells (B). Data from five independent experiments (n = 5) with duplicate measurements. Analysis of samples is done with one-way ANOVA and post hoc Tukey's test (A) or Kruskal-Wallis test and post hoc Dunn's test (B). Levels of significance are indicated as $*p < 0.05$; $**p < 0.01$; $***p < 0.001$ and $****p < 0.0001$.

Consolidation of cell line results was subsequently continued using Western blot analysis. Analogous to J774.2 macrophages (Figure 7A – F), intracellular concentration of NLRP3 inflammasome components and their secretion was partially altered in primary microglia (Figure 10A - F). Elevation of intracellular NLRP3 protein (p = 0.24) and release of cleaved Caspase-1 showed the same tendency when treated with monomeric TDP-43 as in cell lines, although none of the components was upregulated statistically significantly when compared to the untreated control. Of note, induction of NLRP3 inflammasome components by LPS and Nigericin as positive control treatment was also insufficient to exceed the significance threshold except for secretion of cleaved Caspase-1.

Again, CRID3 and IFM were co-applied with TDP-43 proteins to specifically inhibit the NLRP3 inflammasome. In this setting, their inhibitory effect only reached the threshold of significance for cleaved Caspase-1 after positive control treatment with LPS and Nigericin.

Apart from that, an inhibitory effect of IFM might be seen for cleaved Caspase-1 when concomitantly treated with pure monomeric TDP-43 (Figure 10F).
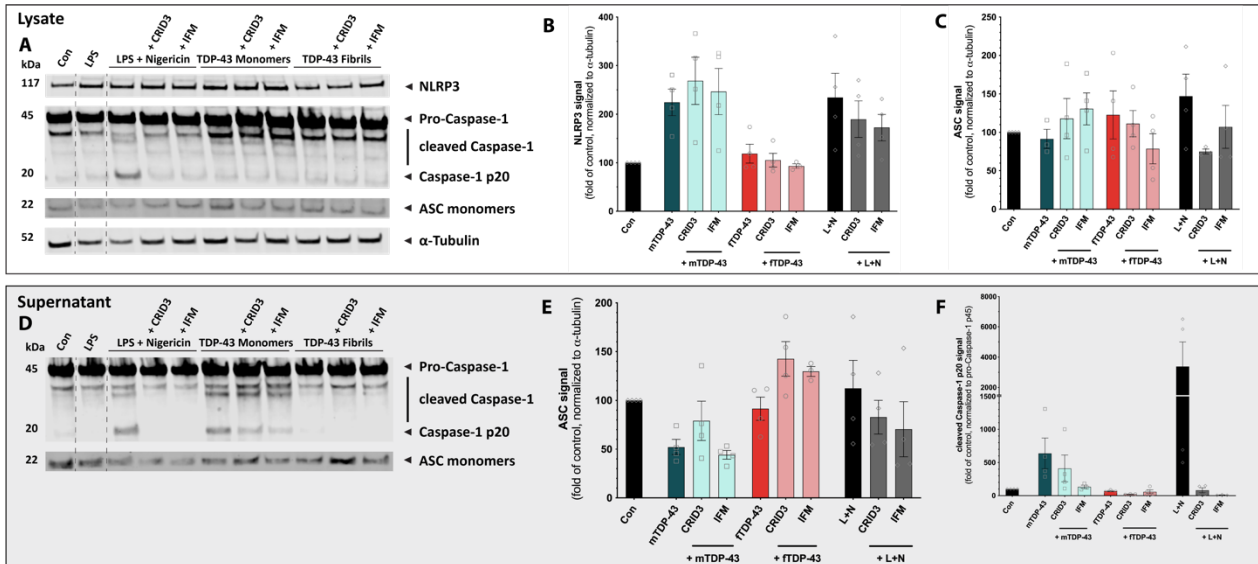

Fig. 10: Induction of NLRP3 inflammasome components by TDP-43 protein in primary microglia

Western blot analysis and quantification of stimulated PMG. Dotted vertical lines indicate spliced sections. Only data used for this project is shown. Quantification of the inflammasomal components NLRP3 (B), ASC (C and E) and cleaved Caspase-1 (F). Cells were seeded at a density of 1×10^6 cells/well in 12-well plates. TDP-43 monomers/ fibrils (mTDP/ fTDP; 100 nM, 24 h) and NLRP3-inflammasome inhibitor (CRID3 or IFM, 1 µM) were used as treatment. LPS (L; 3 h, 100 ng/ml) and Nigericin (N; 1 h, 5 µM) was used as a positive control. Data results from four independent experiments (n = 4). All graphs are displayed as mean ± SEM. Analysis of samples is done with one-way ANOVA and post hoc Tukey's test. Levels of significance are indicated as $*p < 0.05$; $**p < 0.01$; $***p < 0.001$ and $****p < 0.0001$.

Consistent with data from J774.2 macrophages continuative analysis of specimen from Western blot experiments using ELISA were indicative for NLRP3 inflammasome involvement (Figure 11A). A clear difference between TDP-43 monomers and fibrils was found, as IL-1β secretion showed high values after exposure to monomeric TDP-43, while fibrils were not capable to alter protein levels in cell supernatants. As in cell lines, the co-incubation with IFM or CRID3 led to a reduced IL-1β release when used together with TDP-43 monomers. Completing the analysis, investigation of cytotoxicity through an LDH assay showed unaltered values both under peptide treatment and control conditions (Figure 11B).
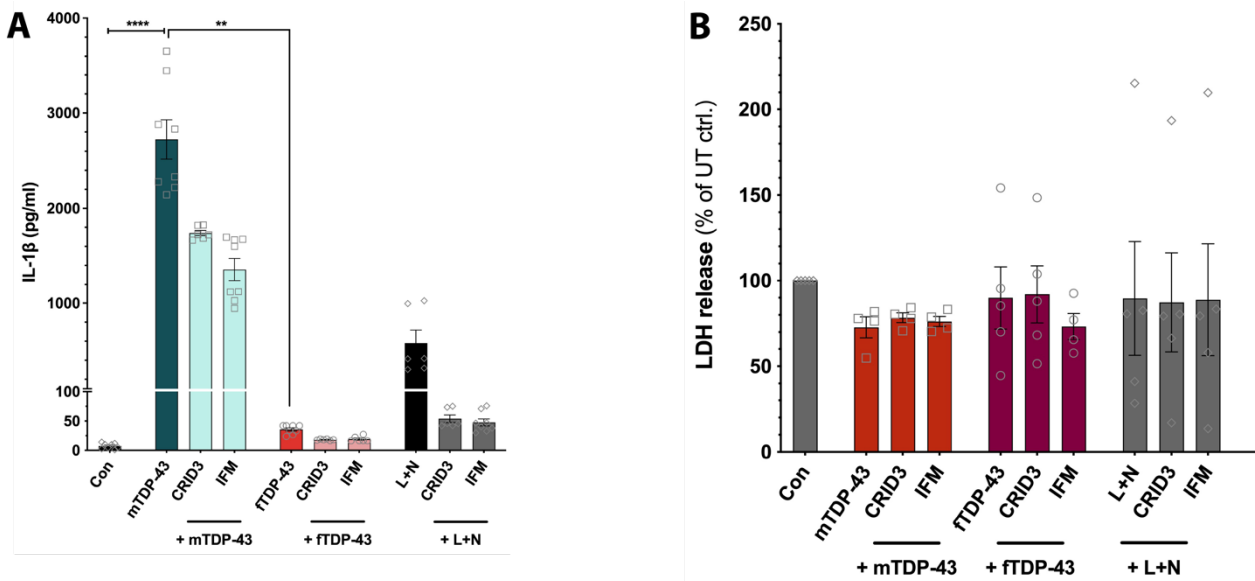
Fig. 11: IL-1β secretion and cytotoxicity after TDP-43 exposure of primary microglia

(A) IL-1β ELISA of supernatant from Western Blot experiments. (B) LDH assay from cell supernatant. Sample preparation as in Figure 10. Analysis of samples is done with Kruskal-Wallis test and post hoc Dunn's test. Levels of significance are indicated as *p < 0.05; **p < 0.01; ***p < 0.001 and ****p < 0.0001.

3.4 Toll-like receptors are involved in sensing TDP-43 and trigger a variety of inflammatory responses

Besides the effects on the NLRP3 inflammasome, the involvement of Toll-like receptors (TLRs) was analyzed using specific anti-TLR antibodies against TLR 2, 4 and 5. Experiments were performed in both J774.2 macrophages and primary microglia.

Secretion of IL-1β into the supernatant was measured by ELISA readout and both cell types showed a significant decrease when TLR antibodies were co-incubated (Figure 12A + C). For macrophages, this effect was particularly strong for TLR 4 blockade, but also anti-TLR 2 and anti-TLR 5 antibodies lead to a significant decrease in cell activation. In primary microglia, the effect of TLR 4 and -5 blockade on IL-1β secretion was attenuated, while blocking TLR 2 still significantly decreased levels in the supernatant as compared to sole exposure to monomeric TDP-43. Interestingly, addition of anti-TLR4-antibody to this setting led to synergistic diminution of IL-1β. Moreover, cell viability was measured with XTT and MTT assays respectively. As in dose-response experiments (Figure 6B +

9B), metabolic activity of cells was much higher for monomeric TDP-43 and TLR-antibody treatment as under control conditions (Figure 12B + D). Especially a co-incubation of monomeric TDP-43 protein and TLR 4-antibody in cell line experiments lead to increased metabolic activity in cell supernatants.
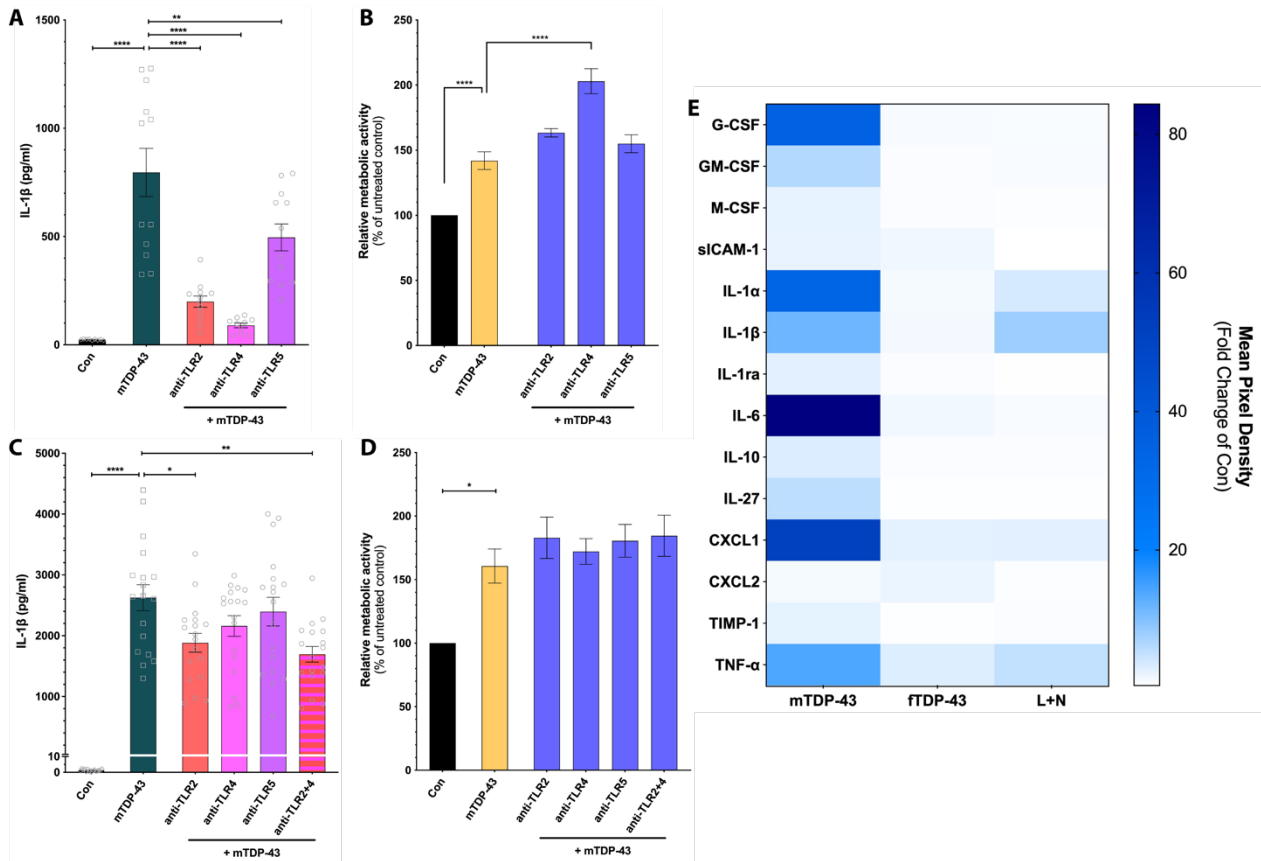

Fig. 12: Involvement of Toll-like receptors and triggered inflammatory responses after sensing of TDP-43

(A + B) Stimulation of J774.2 cells (7.5 x 10^4 cells/ well) with TDP-43 monomers (mTDP; 100 nM, 24 h) with or without TLR 2, 4 and 5 antibodies (5 µg/ml). IL-1β ELISA of supernatant (A) and XTT-assay of stimulated cells (B). (C + D) Stimulation of primary microglia (7.5 x 10^4 cells/ well) with TDP-43 monomers (mTDP; 100 nM, 24 h) and TLR-antibodies (same details as for A + B). IL-1β ELISA of supernatant (C) and MTT-Assay of stimulated cells (D). (E) Heat map from cytokine array of PMG cell supernatant from Western Blot experiments (Figure 10). J774.2 macrophage data from four independent experiments (n = 4) with triplicate measurements (N = 12). PMG data from nine independent experiments (n = 9) with duplicate measurements (N = 18). All graphs are displayed as mean $\pm$ SEM. Analysis of samples is done with one-way ANOVA and post hoc Tukey's test. Levels of significance are indicated as *p < 0.05; **p < 0.01; ***p < 0.001 and ****p < 0.0001.

To characterize the inflammatory potential of TDP-43 protein species in primary microglia more broadly, a Mouse Cytokine Array was used to quantify a large range of mediators simultaneously. Results showed a strong upregulation of various inflammatory proteins when exposed to monomeric but not to fibrillary TDP-43 (Figure 12E). These included chemokines such as TNF-α, IL-1α, IL-1β, IL-6, G-CSF and CXCL1. On the other hand, it is important to note that positive control treatment with LPS and Nigericin induced inflammatory mediators such as IL-1α, IL-1β and TNF-α more specifically compared to TDP-43 monomers. Lastly, with fibrillary TDP-43 only a slight increase of primarily TNF-α and CXC1 was seen.

3.5 Early apoptosis of primary microglia is a result of monomeric TDP-43 treatment

To determine whether treatment with TDP-43 protein species is a possible trigger for pyroptosis via the NLRP3 inflammasome, a FLICA-Assay for active Caspase-1 with subsequent FACS analysis was used. Using fluorochrome-labeled caspase inhibitors (FLICA) and propidium iodide, four specific groups of cells were defined after stimulation with the respective compounds: live (FLICA-/PE-), early apoptotic (FLICA+/PE-), late apoptotic (FLICA+/PE+) and necrotic (FLICA-/PE+).

While only a small percentage of TDP-43 treated cells reached a late apoptotic or a necrotic state, a remarkable discrepancy between simulation with monomeric and fibrillary isoforms was found for early apoptosis (Figure 13A + B). TDP-43 monomers were able to induce early apoptosis in a significant number of cells (33 %). In contrast, treatment with TDP-43 fibrils did not differ from negative controls. As expected, the specific NLRP3 inflammasome activation with LPS and Nigericin lead to a strong activation of caspase-1, which is mirrored by a high proportion of cells reaching an early (77 %) and even a late apoptotic (8 %) state. In parallel, co-incubation of CRID3 with stimulated cells only provoked a subtle dampening in cell activation by monomeric TDP-43, whereas the inhibiting effect was clearly shown for positive control treatment.
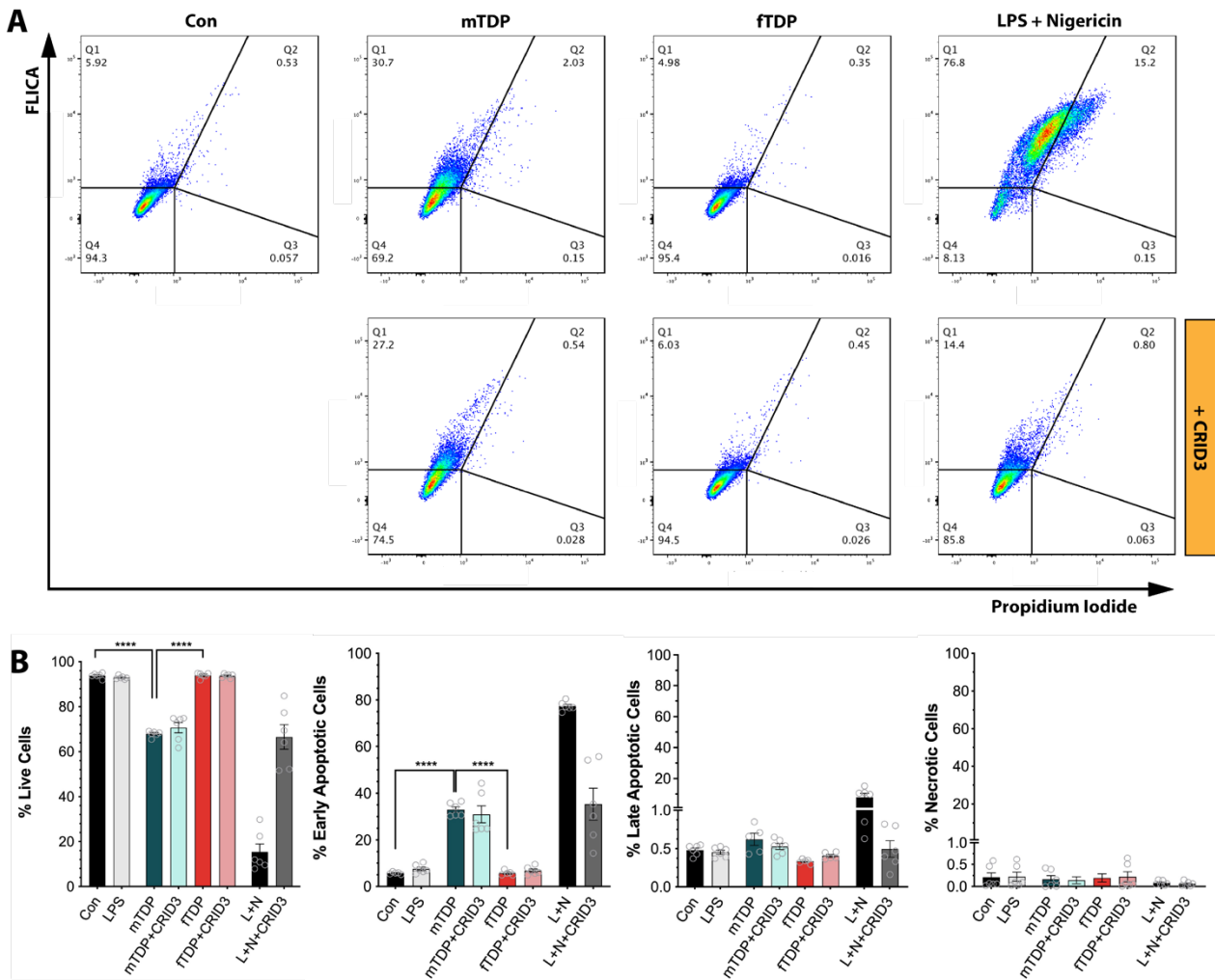
Fig. 13: Quantification of apoptosis of primary microglia upon TDP-43 treatment

(A) FACS analysis of stimulated microglia using FLICA Caspase-1 assay. Stimulation with either TDP-43 monomers or fibrils (mTDP/ fTDP; 100 nM; 24 h) with or without NLRP3 inflammasome inhibitor (CRID3, 1 µM). LPS (3 h, 100 ng/ml) and Nigericin (1 h, 5 µM) was used as a positive control. (B) Quantification of FLICA results distinguishing between different stages of cell death: FLICA-/PE- as live, FLICA+/PE- as early apoptotic, FLICA+/PE+ as late apoptotic and FLICA-/PE+ as necrotic. Data is shown from three independent experiments (n = 3) with duplicate measurements (N = 6) and is displayed as mean ± SEM. Analysis of samples is done with one-way ANOVA and post hoc Tukey's test. Levels of significance are indicated as ****$p < 0.0001$.

3.6 TDP-43 protein can be found within microglial cells in human ALS patients

To hold an eye upon *in vivo* situation, signs of microglial activation were investigated in *post-mortem* brain tissue from patients with TDP-43-positive sporadic ALS. Here, analysis of the two generally most affected regions of the central nervous system in ALS pathology

was performed, the cerebral motor cortex and the ventral grey matter section of the spinal cord. In addition, cerebellar tissue served as a reference to these areas due to its generally lower involvement in TDP-43 pathology (Prell and Grosskreutz, 2013). The respective paraffin-embedded tissue sections were stained for TDP-43, microglial cells (Iba-1) and DAPI.

Microglia together with TDP-43 protein were present in all three regions tested and particularly frequent in the precentral gyrus and anterior horn of thoracal spinal cord (Figure 14A). Furthermore, it is very important to note that TDP-43 protein aggregates were found within the cytosol of microglial cells in many cases. This is exemplarily shown for an Iba-1 positive cell of the gyrus precentralis using z-stack confocal imaging and 3D reconstruction for better visualization (Figure 14B). Above and beyond, TDP-43 protein was also seen in cerebellar tissue sections yet to a much lesser extent.
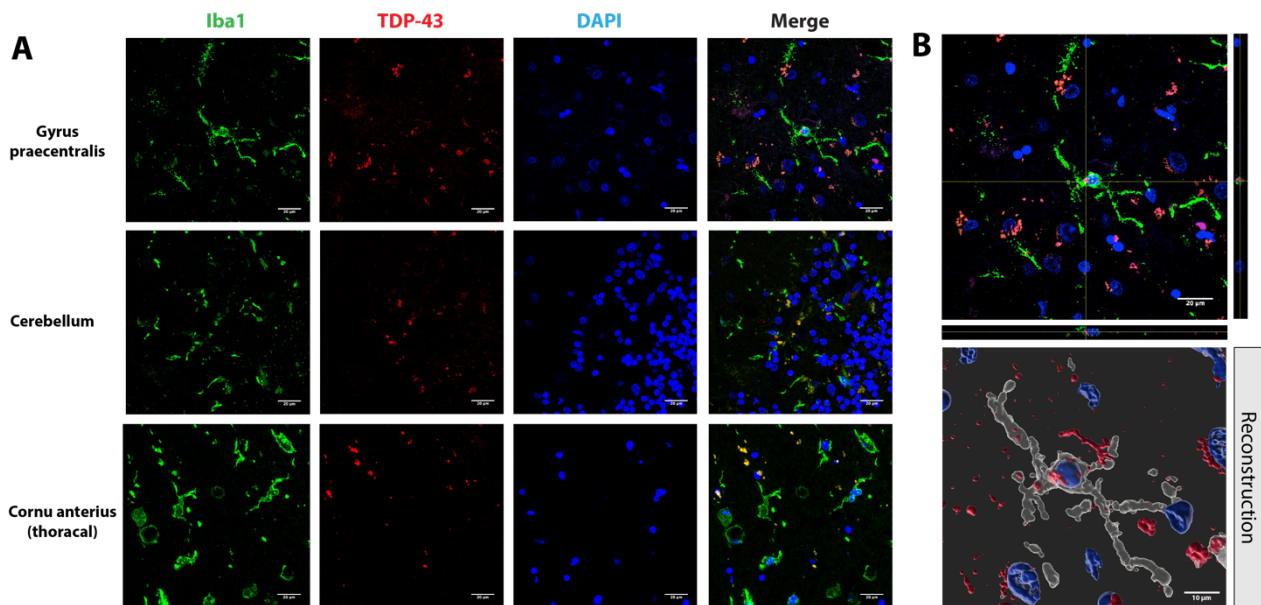

Fig. 14: TDP-43 protein is prevalent in microglial cells of human ALS patients

(A) Confocal microscopy of paraffin-embedded tissue from TDP-43^{+} sporadic ALS-patients. Scale bar 20 µm. (B) Z-Stack of paraffin-embedded tissue from TDP-43^{+} sporadic ALS-patient (top) and its 3D reconstruction (bottom). Scale bars 20 µm (z-stack) and 10 µm (reconstruction).

4. Discussion

ALS as the most common form of MND in adults is far from being sufficiently understood. Patients are still faced with a poor prognosis due to rapid disease progression and ineffective therapeutic options. In this context, a solid basis for novel strategies can only be achieved by constant progress in scientific research. Previous findings have predominantly implicated a disturbed RNA metabolism, altered protein homeostasis and non-cell autonomous toxicity as important drivers of disease pathology (Taylor et al., 2016). Especially for non-cell autonomous toxicity microglia play a fundamental role in many neurological diseases as they are part of the innate immune defense (Ilieva et al., 2009; Liu and Wang, 2017). Since they react to aberrant molecules, it is of particular interest to characterize their initial activating substances in the best possible way. This is also reflected in the fact that it is precisely this neuroinflammatory component of disease development that has increasingly become the focus of scientific interest in recent years (Dorothée, 2018).

Here, I tested the hypothesis that TDP-43 can act as a DAMP and activates the NLRP3 inflammasome. Even though TDP-43 protein has been identified as a pivotal component to initiate the complex process of neuroinflammation, the majority of previous research focuses on mutated or modified forms (Tan et al., 2017). As >95 % of ALS cases do not show mutations in the TDP-43 gene, while cytosolic inclusions of TDP-43 protein are a typical feature of >97 % of ALS patients, it is compelling to further elucidate the neuroinflammatory potential of unaltered wildtype forms (Prasad et al., 2019). This is especially the case for its differentially aggregated forms, where a corresponding examination has so far not been made. As a more profound understanding of ALS pathogenesis is urgently needed, this inequality was addressed by distinction between the two forms initiating and terminating the described sequence, monomers and fibrils. For the stated reasons, I used wild-type full-length TDP-43 protein in its monomeric and fibrillary form to investigate their ability to induce an inflammatory response in immune cells with special focus on the NLRP3 inflammasome.

4.1 Activation of the NLRP3 inflammasome by TDP-43 protein in immune cells

After morphological analysis and verification of monomeric and fibrillary TDP-43 samples, the next step was to gain insights into their stimulatory effects. This was initially done with J774.2 macrophages by dose-dependent exposure to the respective peptides. Here, the secretion of IL-1β was used as a surrogate marker for the NLRP3 inflammasome, as it is formed in the final step of its activation. Clearly results showed a strong difference between TDP-43 monomers and fibrils. While the treatment with monomers led to strong and dose-dependent upregulation of IL-1β, values reached by fibrils did not differ from the untreated control. Interestingly, the highest levels of IL-1β secretion were not reached with the maximum dose of TDP-43 monomers, which might indicate a ceiling effect of macrophage stimulation (Figure 6A).

It is of further importance that production of IL-1β is not entirely specific to the NLRP3 inflammasome alone, but can also result from non-caspase-1 dependent processes (Dinarello, 2018). Consequently, targeted inhibition of the NLRP3 inflammasome with CRID3 gives more detailed information about the underlying signaling pathways. As co-incubation of CRID3 caused lower IL-1β secretion than exposure to TDP-43 monomers alone, this data strongly suggests the involvement of the NLRP3 inflammasome. However, the diminishing effects of CRID3 varies significantly between peptide treatment and positive control. It is clearly visible that the potential to reduce IL-1β secretion is more pronounced for LPS and Nigericin, where IL-1β levels are almost entirely eliminated. Besides a pharmacologically limited effect of CRID3, alternative IL-1β sources induced by TDP-43 monomers are conceivable explanations for this phenomenon.

Besides J774.2 cells, dose-response experiments with TDP-43 monomers and fibrils were also performed using primary microglia. Consistent with data from cell lines, an impressively distinct immunological potential was observed for monomeric and fibrillary isoforms. IL-1β secretion was dose-dependently increased after incubation with TDP-43 monomers, while values reached by fibrils were magnitudes smaller (Figure 9A). Upon closer inspection, a stimulatory tendency was also revealed for fibrils which might display a neuroinflammatory potential at much higher concentrations. With the addition of IFM as a

second NLRP3 inflammasome inhibitor previous results were solidified, emphasizing the likely involvement of the NLRP3 inflammasome into induced metabolic pathways.

To consolidate ELISA-based results, an evaluation by Western blot followed where specific antibodies for all three components of the NLRP3 inflammasome (NLRP3, ASC and Caspase-1) were used. In comparison to a quantitative ELISA read-out, Western blot analysis delivers qualitative results which makes it essential to evaluate the processing of NLRP3 components, especially cleaved caspase-1 as its final effector molecule (Zito et al., 2020). Above that and to precisely determine the NLRP3 inflammasome pathway, the localization of measured components is of special interest. This is attributable to the fact that both ASC and cleaved caspase-1 are secreted only upon actual NLRP3 inflammasome activation (Boucher et al., 2018). Additionally, the cytosolic level of NLRP3 contributes to a comprehensive quantification. Keeping that in mind, the stimulation of J774.2 cells again demonstrated the inflammatory potential of TDP-43 monomers, whereas fibrils proved to be inert. Besides the cytosolic concentration of ASC, all relevant components were significantly elevated (Figure 7). This result does not come unexpectedly, since the lack of an increased cytosolic ASC concentration could mirror its observed secretion. Moreover, the efficacy of both tested NLRP3 inflammasome inhibitors underpinned the data collected, revealing a marginally stronger effect of IFM. The fact that upregulation of NLRP3 protein was not impaired significantly by inhibitory compounds could be explained considering their mechanism of action, which is inhibiting NLRP3 inflammasome oligomerization and activation, while not affecting the translation of its respective components (Figure 7B) (Coll et al., 2019).

Data from primary microglia were not as definite as with cell line findings. Although NLRP3 protein upregulation and elevated secretion of cleaved caspase-1 showed the same tendency after monomeric TDP-43 treatment, data points did not reach the level of significance (Figure 10). While reaching this threshold is not unlikely with a higher number of replicate experiments, a more in-depth interpretation should be omitted at this point. At the same time, this fact makes a closer look at the IL-1β ELISA experiments interesting which were performed from the same material as Western blot analysis. Here, all major findings were confirmed, namely differential response between monomers and fibrils and efficacy of NLRP3 inflammasome inhibitors CRID3 and IFM (Figure 11A). In the context

of data from Western blot analysis, a joint evaluation of these results is highly indicative for NLRP3 inflammasome activation.

Further verification of NLRP3 inflammasome involvement was obtained by analysis of TDP-43's potential to induce an apoptotic effect. This was done by probe-based FACS analysis, quantifying both active caspase-1 and propidium iodide using a FAM-FLICA Caspase-1 assay. As PI positivity reflects a compromised plasma membrane integrity, it was possible to determine cell groups with distinct apoptotic stages. Under concurrent consideration of caspase-1 and PI, early and late apoptosis, as well as necrosis, could therefore be distinguished and differentiated from living cells. After exposure of primary microglia to monomeric or fibrillary TDP-43 respectively, it was shown that early apoptosis is induced by monomeric, but not fibrillary TDP-43 protein (Figure 13). At the same time only a small percentage of stimulated cells entered a late apoptotic stage, whereas necrosis was almost entirely absent. While this reflects an upregulation of active caspase-1 for a considerable amount of the cells, plasma membrane integrity was almost entirely sustained. These findings mirror the data acquired from LDH-assays of Western blot material from both J774.2 macrophages and primary microglia, where unaltered values after monomeric TDP-43 treatment were found (Figure 8B + 11B). As the cytoplasmic enzyme LDH is released into extracellular space in case of a disturbed cell membrane integrity, lacking increase of extracellular concentrations implies a persistent plasma membrane irrespective of high metabolic activity (Kumar et al., 2018).

Surprisingly, specific NLRP3 inflammasome inhibitors did not significantly lower caspase-1 activity in the set of FACS experiments. Detailed examination reveals only a marginally suppressive effect in comparison to sole incubation with TDP-43 monomers. It should be noted however, that the effect of CRID3 on positive control treatment with LPS and Nigericin was also not as strong as in ELISA or Western blot experiments. Once again, this might be due to other sources of active caspase-1 besides the NLRP3 inflammasome. It also points in the same direction as findings from already discussed dose-response experiments where IL-1β secretion was not entirely reduced by specific NLRP3 inflammasome inhibition.

In summary, the data presented provide evidence that the NLRP3 inflammasome is involved in induced metabolic pathways upon exposure to the monomeric, but not fibrillary form of TDP-43 protein. As the blockade of NLRP3 inflammasome assembly is a promising target for many neurodegenerative diseases with chronic inflammation, it is of special interest that both CRID3 and IFM were able to alleviate the detrimental response of microglia and macrophages towards monomeric TDP-43 in most sets of experiments. The importance of possible instruments to control NLRP3 inflammasomal and therefore microglial activation is strengthened by recent findings that degeneration of motor neurons in an ALS mouse model can be recovered in the presence of healthy microglial cells (Spiller et al., 2018). On the other side it is well established that overactivation of the very same cells can result in irreversible tissue damage of the CNS. The adequate reaction of microglia is therefore considered as a double-edged sword, able to tilt the fulcrum of beneficial inflammatory response towards an aggravating metabolic state. As NLRP3 inflammasome inhibitory compounds proved to be possible instruments to control this critical homeostasis, these findings are in line with reports made by Deora et al. (2020) and Zhao et al. (2015) both showing NLRP3 inflammasome-dependent activation of microglia by ALS protein species. To put it in a nutshell, the data obtained underpin the role of TDP-43 protein species in ALS pathology and gives hope for NLRP3 inflammasome blockade as a possible target of a therapeutic approach in ALS.

4.2 Contribution of other immune mediators to TDP-43 stimulation

Although the NLRP3 inflammasome has been widely implicated in neuroinflammation and is among the best studied molecular hubs, it is important to keep an eye also upon other secreted mediators of inflammation (for review see: Péladeau and Sandhu, 2021). It is therefore not surprising that metabolic stimulation by monomeric TDP-43 was not limited to NLRP3 inflammasome activation and secretion of IL-1β. Primary microglia strongly upregulated a wide variety of inflammatory cytokines including TNF-α and IL-6 as two typical proinflammatory mediators promoting neuroinflammation (Erta et al., 2012; Rizzo et al., 2018). In a chemokine array IL-6 (84-fold), CXCL1 (52-fold), G-CSF (34-fold) and IL-1α (33-fold) were the most elevated cytokines (Figure 12E). Interestingly, previous research

has linked all these mediators in a certain degree to neuroinflammation, which underlines the capability of monomeric TDP-43 to act as a DAMP (Lepennetier et al., 2019). This broad spectrum of induced mediators is reflected by data from XTT and MTT cell viability assays where metabolic activation was quantified. For both J774.2 macrophages and primary microglia values were high after treatment with monomeric TDP-43 in a dose-dependent manner and unaltered when TDP-43 fibrils were used (Figure 6B + 9B). Elevated levels could only be reduced partly by NLRP3 inflammasome inhibitors which corroborates that a wide variety of signaling pathways are involved in the inflammatory response to TDP-43 protein. For completeness, it should be noted that the sequential treatment of LPS and Nigericin did not cause an increase in metabolic activity, but even diminished it in the case of primary microglia. These results are likely to be related to the strong pyroptotic effect of these compounds, which accounts for a reduced quantity of activated, but living cells (den Hartigh et al., 2018).

In addition, it is demonstrated that J774.2 macrophage and primary microglial activation is dependent on different Toll-like receptors. As already mentioned, TLRs are cell surface receptors acting as PRRs, thus implicated in the detection of PAMPs and DAMPs that originate from diverse sources. It is shown that TLR 2, TLR 4 and TLR 5 are all involved in sensing monomeric TDP-43 molecules with a stronger contribution of TLR 2 and TLR 4 (Figure 12). For primary microglia a concomitant inhibition of TLR 2 and TLR 4 during treatment with TDP-43 monomers revealed synergistic effects. This is in line not only with the fact that TLR 2 and TLR 4 are particularly capable to recognize diverse molecular patterns, but also with previous research showing that NF-κB, as well as CD14 are part of induced signaling pathways by TDP-43 peptides (Bauernfeind et al., 2009; Kawasaki and Kawai, 2014; Mukherjee et al., 2016). CD14 acts as a co-receptor of TLR 4 and TLRs are known to induce NF-κB (Zanoni et al., 2011). Likewise, this data provides a link to the NLRP3 inflammasome, as the described sequence is part of NLRP3 inflammasome priming (Heneka et al., 2018). This fact is of eminent importance and could reflect the ability of TDP-43 not only to activate, but also to prime the NLRP3 inflammasome via the respective TLRs. Assuming this is accurate, this would be the first demonstration of these capabilities for TDP-43 and thus for ALS.

As both macrophage cell lines and primary microglia were tested, it was searched for possible differences of TLR-inhibitory effects. Indeed, murine J774.2 macrophages showed a more pronounced diminution of IL-1β secretion when TLRs were blocked than primary microglia. Nonetheless, levels of detected IL-1β secretion were still significantly reduced after anti-TLR 2 treatment in primary microglia as well as for simultaneous blockade of TLR 2 and TLR 4. Even though the release of IL-1β into cell supernatants was partly impaired, levels of metabolic activation persisted on a high level after blockade of TLRs as can be seen in consecutively performed XTT and MTT assays. In fact, cell viability experiments showed even increased results when anti-TLR 4 antibodies were co-incubated with monomeric TDP-43 in J774.2 macrophages. Once more, these data demonstrate that the tested signaling pathways are not the only culprits that account for an inflammatory response of immune cells after TDP-43 stimulation. Nonetheless, the involvement of TLRs in the induced metabolic pathways of TDP-43 protein species represents another essential component to unravel its toxic properties. It not only supports previous research findings, but also puts the basis for a more detailed analysis.

4.3 Limitations of this study

The informative value of this thesis is primarily limited by a possibly restricted transferability to the human organism. As experiments were mainly performed in murine experimental models, it is conceivable that human microglia react differently to TDP-43 protein species and that induced pathways may vary. To dampen this discrepancy the analysis of human *post-mortem* material from the central nervous system of sporadic ALS patients was included in this study. Here, both a high density of TDP-43 protein aggregates and microglia were present in all examined CNS regions. The microglial cells were found not only clustering around these aggregates, but even showed cytosolic deposits (Figure 14). Despite the demonstrated presence of TDP-43 deposits, these findings only present the first step in a cascade of necessary experiments to determine the neurotoxic properties of TDP-43 protein *in vivo*.

Furthermore, TDP-43 protein samples were synthesized by our collaborators using an *Escherichia coli*-based expression platform. As a residuum of recombinant protein production in Gram-negative bacteria, the existence of low levels of endotoxin cannot be fully excluded as purification is challenging and expensive (Mamat et al., 2015; Wakelin et al., 2006). Since this study aims to analyze the inflammatory response of immune cells, it is eminent to consider endotoxin as a confounder, especially as residual contaminations were able to activate immune cells in distinct experimental settings (Schwarz et al., 2014). For this study, TDP-43 monomers and fibrils were both synthesized by the same bacteria and under the same conditions which makes endotoxin-based differences between these isoforms highly unlikely. Nonetheless, slight differences in the immunologic potential might be due to remaining levels of endotoxin.

Another important fact is the difficulty to assess whether the tested concentrations are in line with interstitial TDP-43 levels of ALS-affected individuals. Previous scientific studies focused on CSF and blood plasma concentrations of TDP-43, where significantly lower protein concentrations were found (Kasai et al., 2009; Verstraete et al., 2012). As a logical consequence, much higher peptide concentrations should be expected in CNS parenchyma, as protein aggregates originate here and have not been diluted. However, reliable data on interstitial concentrations do not yet exist and one can only speculate about their actual level. Still, it is precisely this figure which is needed to adequately evaluate the tested peptide concentrations in the real context of ALS pathology, since this is the place where microglia come into contact with TDP-43 protein. As a reference, the peptide levels used were intermediate between the concentrations of two previous studies from Deora et al. (2020) and Zhao et al. (2015) that investigated TDP-43 in a similar approach.

Lastly, it is important to bear in mind that immune cells were not primed with LPS prior to the stimulation with TDP-43 protein. While it is widely accepted that the activation of the NLRP3 inflammasome requires a preceding priming step to upregulate inflammasomal components and other immunologic mediators, more recent studies also reveal canonical NLRP3 inflammasome activation in the absence of priming (de Carvalho et al., 2019; Gritsenko et al., 2020). Above that, current data from Scheiblich et al. (2021) reveal that some neurotoxic protein species are even capable to both prime and activate the NLRP3 inflammasome. As the data of this study not only proves that TLRs are part of induced

signaling pathways but also that the NLRP3 inflammasome becomes activated, a similar effect is suggested for TDP-43 monomers. If accurate or not, the exposure to distinct acute inflammatory mediators acting as DAMPs and PAMPs in human CNS parenchyma of ALS patients is likely to potentize the metabolic pathways and responses analyzed in this study.

4.4 Avenues for further studies or analyses

Transfer of *in-vitro* and animal data into the human conditions is not straightforward. While this study tries to overcome this discrepancy by a three-step approach including brain sections of ALS-affected individuals, further research is needed to confirm and expand these results. Despite immense efforts, the perfect system to fill the gap between primary macrophages from human and amenability for genetic alteration and replicability is still lacking (Zito et al., 2020). Yet various cellular models aim to combine these properties in the best possible way. One option to confirm the obtained data would be the use of primary microglial cells from knock-out mice. With regard to TDP-43, this could be done using the same techniques as in a variety of other neuroinflammation studies, namely knock-out of NLRP3 inflammasome components or modification of specific TLR genes (Fang et al., 2019; Qin et al., 2021; Tejera et al., 2019). Other promising possibilities to investigate the interplay between TDP-43 and neuroinflammation, thereby extending the content of this study, might include murine bone marrow-derived macrophages (BMDMs) or human mon-ocyte-derived macrophages (hMDMs). Especially BMDMs have emerged as an effective and financially feasible method in the field of macrophage research (Bailey et al., 2020; Marim et al., 2010; Zito et al., 2020). The fact that they can be obtained from knock-out mice makes them even more valuable for further scientific studies. Last but not least, more detailed diagnostics directly with human tissue would be suitable to further substantiate and deepen the obtained data. Key points of these examinations would include the use of thicker tissue sections to yield better morphological visualization, as well as Western blot analyses for extended qualitative evaluation of NLRP3 inflammasome components and induced signaling pathways.

To further elucidate the involvement of the NLRP3 inflammasome upon stimulation with TDP-43, several approaches could be usefully employed. Despite recent findings challenging the classical conception of two-stage canonical NLRP3 inflammasome activation, the vast majority of NLRP3 inflammasome studies still follows this principle (Deora et al., 2020; Friker et al., 2020; Ising et al., 2019). As cells used in this study were exposed to sole TDP-43 proteins, future studies could include a priming step with LPS. This would also shed light on the possible capability of TDP-43 monomers to both prime and activate the NLRP3 inflammasome. Notwithstanding this approach, specific protocols could be used to further characterize the induced components. This is especially applicable to ASC, which can aggregate into large protein aggregates culminating in so-called ASC specks, which serve as an upstream read-out of NLRP3 inflammasome activation (Stutz et al., 2013). This would be of particular relevance as ASC showed ambiguous findings in some of the experiments performed with primary microglia (Fig. 7C + E). To address this, possible starting points would be the use of alternative antibodies but especially the implementation of ASC cross-linking protocols, which are capable to distinguish between differently aggregated isoforms of ASC (Lugrin and Martinon, 2017).

On another level, future analyses might extend the spectrum of TDP-43 aggregates to their entirety, with a special focus towards oligomers and protofibrils. Keeping in mind that it is especially these two isoforms which exhibit neurotoxic properties in AD and PD, it is not unlikely that future studies will reveal similar characteristics also for ALS (Alam et al., 2019; Lučiūnaitė et al., 2020). In this respect, stimulation of immune cells with higher concentrations of TDP-43 fibrils likewise could complement this picture in another direction. Considering the marginal but dose-dependent immunostimulatory effect on primary microglia (Figure 6A), a neurotoxic effect at elevated levels would be conceivable. On the whole, a precise molecular understanding of TDP-43's neurotoxicity is not only important for a detailed comprehension of ALS pathophysiology, but is also indispensable to efficiently target relevant molecules and pathways. Given the urgent requirement of pharmaceutical options to ameliorate ALS progression, this knowledge could play its role in halting or reversing neurological consequences.

Taking this one step further, inhibition of the NLRP3 inflammasome in ALS patients emerges as a promising therapeutical target. Including the research of this project, an

increasing amount of studies reveal microglial activation and NLRP3 inflammasome involvement in ALS pathology (Deora et al., 2020; Zhao et al., 2015). Moreover, for some diseases with an inflammatory component NLRP3 inflammasome inhibitors are already tested in clinical trials (for summary see: Chen et al., 2021). However, the final results are still pending for most of these studies, leaving the assessment of the respective effect to be awaited.

In summary, this study provides the basis for multiple avenues for future research. Evidence is provided that the NLRP3 inflammasome is induced by TDP-43 protein species and that a profound difference exists between its monomeric and fibrillary isoforms. In addition, microglial activation occurs via the upregulation of a broad variety of intercellular mediators. This is not only the case for IL-1β reflecting NLRP3 inflammasome activation, but also for well-characterized cytokines like IL-6 and TNF-α. Furthermore, it is shown that TLRs are involved in the binding of TDP-43 proteins and trigger intracellular signaling cascades. Here, existing knowledge is expanded to the fact that TLR 2, TLR 4 and TLR 5 are implicated in metabolic processes. This is of particular interest because it may represent another significant neurotoxic capacity of TDP-43, which involves both priming of the NLRP3 inflammasome as well as its activation. To conclude with, early apoptosis of immune cells is revealed as a relevant part of TDP-43's neurotoxic properties.

5. Summary

ALS as one of the most common and aggressive neuromuscular diseases is characterized by rapidly progressing and, in later stages, generalized muscular decline. As of today, limited therapeutic options exist and there is no significant disease modifying therapy. Pathological hallmarks are mislocalized, insoluble cytoplasmic protein aggregates positive for TDP-43 that are prevalent mainly in motor neurons. While disease etiology is complex and remains an enduring enigma, neuroinflammation is emerging as a key player in recent years. Drivers of this process are predominantly microglia, which represent the first line of defense within the CNS. In a self-amplifying manner, their overactivation can account for non-cell autonomous toxicity and exacerbates disease progression. A profound knowledge of underlying mechanisms is therefore of eminent importance.

In this study, I was able to examine in detail the stimulatory potential of TDP-43 protein species as one of the hallmarks in ALS pathology. I report for the first time of the differential effects of monomeric and fibrillary isoforms in both macrophage cell lines and primary microglia and exemplify results using human tissue. Upon stimulation with monomeric TDP-43, the NLRP3 inflammasome, a key regulator of inflammation, is activated and a broad variety of immune mediators are upregulated. These include TNF-α and IL-6 as two prototypical proinflammatory mediators. In addition, the existing knowledge is expanded to the effect that Toll-like receptors are involved in sensing TDP-43 molecules and initiate an intracellular signaling cascade which leads to NLRP3 inflammasome priming and activation provoking early apoptosis. Therefore, the immunologic response towards TDP-43 protein includes, but is not limited to the proposed pathway of TDP-43 regulated NLRP3 inflammasome activation as summarized in Figure 15. Here, I present an overview of how the acquired results can be placed in a bigger picture and brought into accordance with known metabolic pathways.
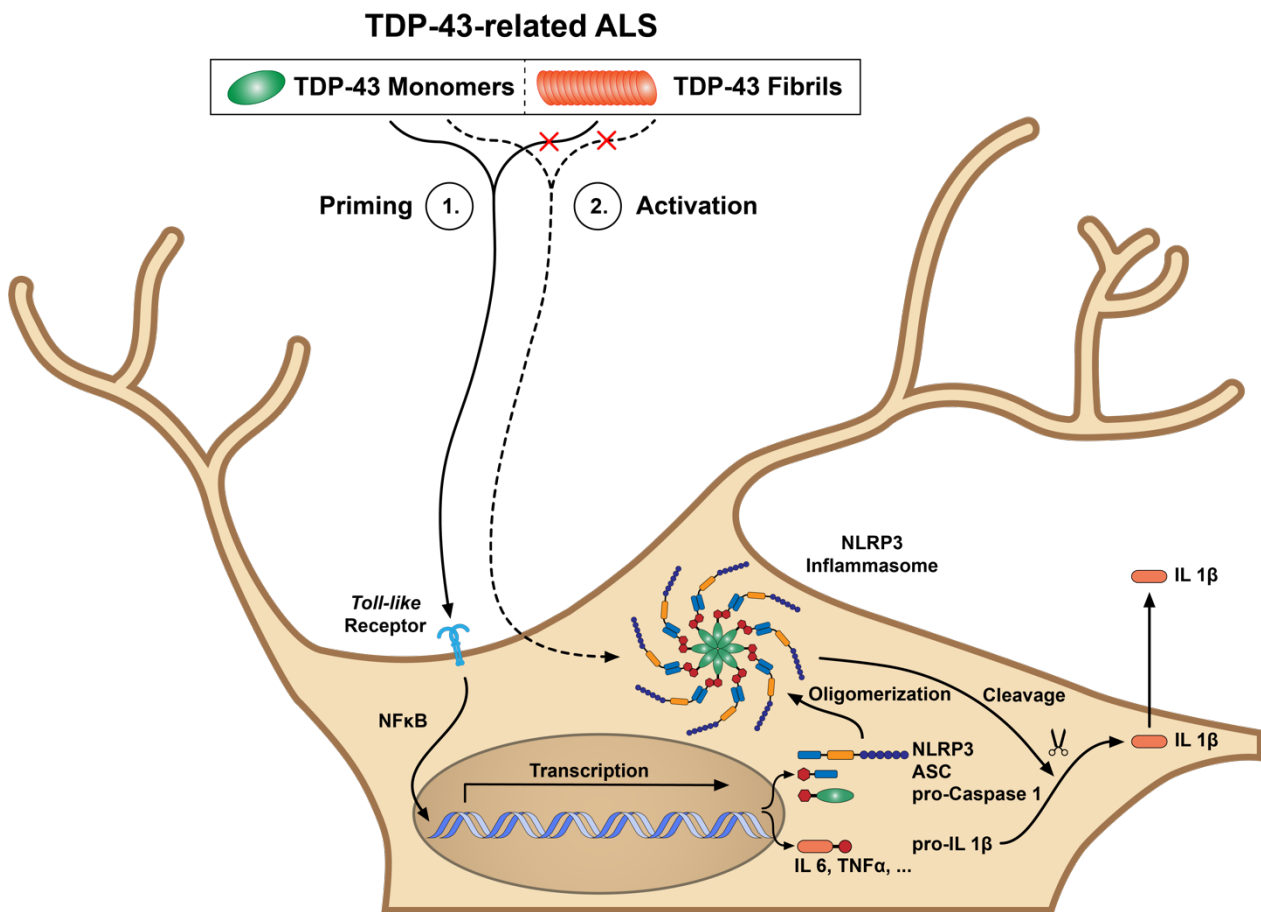
Fig. 15: Induced metabolic pathways by TDP-43 protein species

Schematic showing the proposed pathway of TDP-43 regulated inflammasome reaction. Monomeric but not fibrillary TDP-43 protein triggers NLRP3-inflammasomal priming via Toll-like receptors (TLRs). These receptors activate the NF-κB-pathway and various inflammatory cytokines such as TNF-α and pro-IL-1β and induce the production of components of the NLRP3 inflammasome. After subsequent activation of the NLRP3 inflammasome via TDP-43 monomers, activated IL-1β is released into the interstitium among other upregulated chemokines.

Taken together, the results underline that TDP-43 as an important ALS-associated protein species is a crucial player in ALS pathology, namely the neuroinflammatory process. The data provide evidence that monomeric TDP-43 in its wild-type full-length form can drive neuroinflammation. This raises exciting therapeutic opportunities that need to be explored further.

6. List of figures

7. List of tables

8. References

Abe K, Itoyama Y, Sobue G, Tsuji S, Aoki M, Doyu M, Hamada C, Kondo K, Yoneoka T, Akimoto M, Yoshino H, Edaravone ALS Study Group. Confirmatory double-blind, parallel-group, placebo-controlled study of efficacy and safety of edaravone (MCI-186) in amyotrophic lateral sclerosis patients. Amyotroph Lateral Scler Frontotemporal Degener 2014; 15: 610–617

Alam P, Bousset L, Melki R, Otzen DE. α-synuclein oligomers and fibrils: a spectrum of species, a spectrum of toxicities. J Neurochem 2019; 150: 522–534

Andrews JA, Jackson CE, Heiman-Patterson TD, Bettica P, Brooks BR, Pioro EP. Real-world evidence of riluzole effectiveness in treating amyotrophic lateral sclerosis. Amyotroph Lateral Scler Frontotemporal Degener 2020; 21: 509–518

Arai T, Hasegawa M, Akiyama H, Ikeda K, Nonaka T, Mori H, Mann D, Tsuchiya K, Yoshida M, Hashizume Y, Oda T. TDP-43 is a component of ubiquitin-positive tau-negative inclusions in frontotemporal lobar degeneration and amyotrophic lateral sclerosis. Biochem Biophys Res Commun 2006; 351: 602–611

Arthur KC, Calvo A, Price TR, Geiger JT, Chiò A, Traynor BJ. Projected increase in amyotrophic lateral sclerosis from 2015 to 2040. Nat Commun 2016; 7: 12408

Ayala YM, Zago P, D'Ambrogio A, Xu YF, Petrucelli L, Buratti E, Baralle FE. Structural determinants of the cellular localization and shuttling of TDP-43. J Cell Sci 2008; 121: 3778–3785

Bailey JD, Shaw A, McNeill E, Nicol T, Diotallevi M, Chuaiphichai S, Patel J, Hale A, Channon KM, Crabtree MJ. Isolation and culture of murine bone marrow-derived macrophages for nitric oxide and redox biology. Nitric Oxide 2020; 100–101: 17–29

Barber SC, Shaw PJ. Oxidative stress in ALS: Key role in motor neuron injury and therapeutic target. Free Radic Biol Med 2010; 48: 629–641

Barmada SJ, Skibinski G, Korb E, Rao EJ, Wu JY, Finkbeiner S. Cytoplasmic Mislocalization of TDP-43 Is Toxic to Neurons and Enhanced by a Mutation Associated with Familial Amyotrophic Lateral Sclerosis. J Neurosci 2010; 30: 639–649

Bauernfeind F, Horvath G, Stutz A, Alnemri ES, MacDonald K, Speert D, Fernandes-Alnemri T, Wu J, Monks BG, Fitzgerald KA, Hornung V, Latz E. NF-kB activating pattern recognition and cytokine receptors license NLRP3 inflammasome activation by regulating NLRP3 expression. J Immunol 2009; 183: 787–791

Bergsbaken T, Fink SL, Cookson BT. Pyroptosis: host cell death and inflammation. Nat Rev Microbiol 2009; 7: 99–109

Berning BA, Walker AK. The Pathobiology of TDP-43 C-Terminal Fragments in ALS and FTLD. Front Neurosci 2019; 13

Blevins HM, Xu Y, Biby S, Zhang S. The NLRP3 Inflammasome Pathway: A Review of Mechanisms and Inhibitors for the Treatment of Inflammatory Diseases. Front Aging Neurosci 2022; 14: 879021

Boaru SG, Borkham-Kamphorst E, Van de Leur E, Lehnen E, Liedtke C, Weiskirchen R. NLRP3 inflammasome expression is driven by NF-κB in cultured hepatocytes. Biochem Biophys Res Commun 2015; 458: 700–706

Boucher D, Monteleone M, Coll RC, Chen KW, Ross CM, Teo JL, Gomez GA, Holley CL, Bierschenk D, Stacey KJ, Yap AS, Bezbradica JS, Schroder K. Caspase-1 self-cleavage is an intrinsic mechanism to terminate inflammasome activity. J Exp Med 2018; 215: 827–840

Buratti E. Functional Significance of TDP-43 Mutations in Disease. Adv Genet 2015; 91: 1-53

Cacabelos D, Ramírez-Núñez O, Granado-Serrano AB, Torres P, Ayala V, Moiseeva V, Povedano M, Ferrer I, Pamplona R, Portero-Otin M, Boada J. Early and gender-specific differences in spinal cord mitochondrial function and oxidative stress markers in a mouse model of ALS. Acta Neuropathol Commun 2016; 4: 3

Chang YP, Ka SM, Hsu WH, Chen A, Chao LK, Lin CC, Hsieh CC, Chen MC, Chiu HW, Ho CL, Chiu YC, Liu ML, Hua KF. Resveratrol inhibits NLRP3 inflammasome activation by preserving mitochondrial integrity and augmenting autophagy. J Cell Physiol 2015; 230: 1567-1579

Chanson JB, Echaniz-Laguna A, Vogel T, Mohr M, Benoilid A, Kaltenbach G, Kiesmann M. TDP43-positive intraneuronal inclusions in a patient with motor neuron disease and Parkinson's disease. Neurodegener Dis 2010; 7: 260–264

Chen G, Xu T, Yan Y, Zhou Y, Jiang Y, Melcher K, Xu HE. Amyloid beta: structure, biology and structure-based therapeutic development. Acta Pharmacol Sin 2017; 38: 1205–1235

Chen QL, Yin HR, He QY, Wang Y. Targeting the NLRP3 inflammasome as new therapeutic avenue for inflammatory bowel disease. Biomed Pharmacother 2021; 138: 111442

Chiò A, Logroscino G, Traynor BJ, Collins J, Simeone JC, Goldstein LA, White LA. Global Epidemiology of Amyotrophic Lateral Sclerosis: A Systematic Review of the Published Literature. Neuroepidemiology 2013; 41: 118–130

Cohen TJ, Lee VMY, Trojanowski JQ. TDP-43 functions and pathogenic mechanisms implicated in TDP-43 proteinopathies. Trends Mol Med 2011; 17: 659–667

de Carvalho RVH, Silva ALN, Santos LL, Andrade WA, de Sá KSG, Zamboni DS. Macrophage priming is dispensable for NLRP3 inflammasome activation and restriction of Leishmania amazonensis replication. J Leukoc Biol 2019; 106: 631–640

de Oliviera Nascimento L, Massari P, Wetzler L. The Role of TLR2 in Infection and Immunity. Front Immunol 2012; 3: 79

DeJesus-Hernandez M, Mackenzie IR, Boeve BF, Boxer AL, Baker M, Rutherford NJ, Nicholson AM, Finch NA, Gilmer HF, Adamson J, Kouri N, Wojtas A, Sengdy P, Hsiung GYR, Karydas A, Seeley WW, Josephs KA, Coppola G, Geschwind DH, Wszolek ZK, Feldman H, Knopman D, Petersen R, Miller BL, Dickson D, Boylan K, Graff-Radford N, Rademakers R. Expanded GGGGCC hexanucleotide repeat in non-coding region of C9ORF72 causes chromosome 9p-linked frontotemporal dementia and amyotrophic lateral sclerosis. Neuron 2011; 72: 245–256

Deora V, Lee JD, Albornoz EA, McAlary L, Jagaraj CJ, Robertson AAB, Atkin JD, Cooper MA, Schroder K, Yerbury JJ, Gordon R, Woodruff TM. The microglial NLRP3 inflammasome is activated by amyotrophic lateral sclerosis proteins. Glia 2020; 68: 407–421

Di A, Xiong S, Ye Z, Malireddi RKS, Kometani S, Zhong M, Mittal M, Hong Z, Kanneganti TD, Rehman J, Malik AB. The TWIK2 Potassium Efflux Channel in Macrophages Mediates NLRP3 Inflammasome-induced Inflammation. Immunity 2018; 49: 56-65.e4

Dinarello CA. Overview of the IL-1 family in innate inflammation and acquired immunity. Immunol Rev 2018; 281: 8–27

Dorothée G. Neuroinflammation in neurodegeneration: role in pathophysiology, therapeutic opportunities and clinical perspectives. J Neural Transm (Vienna) 2018; 125: 749–750

Duncan JA, Bergstralh DT, Wang Y, Willingham SB, Ye Z, Zimmermann AG, Ting JPY. Cryopyrin/NALP3 binds ATP/dATP, is an ATPase, and requires ATP binding to mediate inflammatory signaling. Proc Natl Acad Sci U S A 2007; 104: 8041–8046

Erta M, Quintana A, Hidalgo J. Interleukin-6, a Major Cytokine in the Central Nervous System. Int J Biol Sci 2012; 8: 1254–1266

Fang R, Uchiyama R, Sakai S, Hara H, Tsutsui H, Suda T, Mitsuyama M, Kawamura I, Tsuchiya K. ASC and NLRP3 maintain innate immune homeostasis in the airway through an inflammasome-independent mechanism. Mucosal Immunol 2019; 12: 1092–1103

Feldman N, Rotter-Maskowitz A, Okun E. DAMPs as mediators of sterile inflammation in aging-related pathologies. Ageing Res Rev 2015; 24: 29–39

Fitzgerald KA, Kagan JC. Toll-like Receptors and the control of immunity. Cell 2020; 180: 1044–1066

Friker LL, Scheiblich H, Hochheiser IV, Brinkschulte R, Riedel D, Latz E, Geyer M, Heneka MT. β-Amyloid Clustering around ASC Fibrils Boosts Its Toxicity in Microglia. Cell Rep 2020; 30: 3743-3754.e6

Furukawa Y, Kaneko K, Watanabe S, Yamanaka K, Nukina N. A seeding reaction recapitulates intracellular formation of Sarkosyl-insoluble transactivation response element (TAR) DNA-binding protein-43 inclusions. J Biol Chem 2011; 286: 18664–18672

Ghasemi M, Brown RH. Genetics of Amyotrophic Lateral Sclerosis. Cold Spring Harb Perspect Med 2018; 8: a024125

Giannini M, Bayona-Feliu A, Sproviero D, Barroso SI, Cereda C, Aguilera A. TDP-43 mutations link Amyotrophic Lateral Sclerosis with R-loop homeostasis and R loop-mediated DNA damage. PLoS Genet 2020; 16: e1009260

Gitcho MA, Baloh RH, Chakraverty S, Mayo K, Norton JB, Levitch D, Hatanpaa KJ, White III CL, Bigio EH, Caselli R, Baker M, Al-Lozi MT, Morris JC, Pestronk A, Rademakers R, Goate AM, Cairns NJ. TDP-43 A315T mutation in familial motor neuron disease. Ann Neurol 2008; 63: 535–538

Giulian D, Baker T. Characterization of ameboid microglia isolated from developing mammalian brain. J Neurosci 1986; 6: 2163–2178

Global Data Plc, 2022: Number of ongoing Clinical Trials (for drugs) involving Amyotrophic Lateral Sclerosis by Phase; https://www.globaldata.com/data-insights/pharmaceuticals/number-of-ongoing-clinical-trials-for-drugs-involving-amyotrophic-lateral-sclerosis-by-phase-503191/ (access date: 09.04.2022)

Gritsenko A, Yu S, Martin-Sanchez F, Diaz-del-Olmo I, Nichols EM, Davis DM, Brough D, Lopez-Castejon G. Priming Is Dispensable for NLRP3 Inflammasome Activation in Human Monocytes In Vitro. Front Immunol 2020; 11: 565924

Guzman-Martinez L, Maccioni RB, Andrade V, Navarrete LP, Pastor MG, Ramos-Escobar N. Neuroinflammation as a Common Feature of Neurodegenerative Disorders. Front Pharmacol 2019; 10: 1008

Heneka MT, Kummer MP, Latz E. Innate immune activation in neurodegenerative disease. Nat Rev Immunol 2014; 14: 463–477

Heneka MT, McManus RM, Latz E. Inflammasome signalling in brain function and neurodegenerative disease. Nat Rev Neurosci 2018; 19: 610–621

Hergesheimer RC, Chami AA, de Assis DR, Vourc'h P, Andres CR, Corcia P, Lanznaster D, Blasco H. The debated toxic role of aggregated TDP-43 in amyotrophic lateral sclerosis: a resolution in sight?. Brain 2019; 142: 1176–1194

Hirano S, Zhou Q, Furuyama A, Kanno S. Differential Regulation of IL-1β and IL-6 Release in Murine Macrophages. Inflammation 2017; 40: 1933–1943

Hochheiser IV, Behrmann H, Hagelueken G, Rodríguez-Alcázar JF, Kopp A, Latz E, Behrmann E, Geyer M. Directionality of PYD filament growth determined by the transition of NLRP3 nucleation seeds to ASC elongation. Sci Adv 2022; 8: eabn7583

Holbrook JA, Jarosz-Griffiths HH, Caseley E, Lara-Reyna S, Poulter JA, Williams-Gray CH, Peckham D, McDermott MF. Neurodegenerative Disease and the NLRP3 Inflammasome. Front Pharmacol 2021; 12: 193

Igaz LM, Kwong LK, Xu Y, Truax AC, Uryu K, Neumann M, Clark CM, Elman LB, Miller BL, Grossman M, McCluskey LF, Trojanowski JQ, Lee VMY. Enrichment of C-Terminal Fragments in TAR DNA-Binding Protein-43 Cytoplasmic Inclusions in Brain but not in Spinal Cord of Frontotemporal Lobar Degeneration and Amyotrophic Lateral Sclerosis. Am J Pathol 2008; 173: 182–194

Ilieva H, Polymenidou M, Cleveland DW. Non–cell autonomous toxicity in neurodegenerative disorders: ALS and beyond. J Cell Biol 2009; 187: 761–772

Ince PG, Highley JR, Kirby J, Wharton SB, Takahashi H, Strong MJ, Shaw PJ. Molecular pathology and genetic advances in amyotrophic lateral sclerosis: an emerging molecular pathway and the significance of glial pathology. Acta Neuropathol 2011; 122: 657–671

Ingelsson M. Alpha-Synuclein Oligomers—Neurotoxic Molecules in Parkinson's Disease and Other Lewy Body Disorders. Front Neurosci 2016; 10: 408

Ising C, Venegas C, Zhang S, Scheiblich H, Schmidt SV, Vieira-Saecker A, Schwartz S, Albasset S, McManus RM, Tejera D, Griep A, Santarelli F, Brosseron F, Opitz S, Stunden J, Merten M, Kayed R, Golenbock DT, Blum D, Latz E, Buée L, Heneka MT. NLRP3 inflammasome activation drives tau pathology. Nature 2019; 575: 669–673

Jo M, Lee S, Jeon YM, Kim S, Kwon Y, Kim HJ. The role of TDP-43 propagation in neurodegenerative diseases: integrating insights from clinical and experimental studies. Exp Mol Med 2020; 52: 1652–1662

Kabashi E, Valdmanis PN, Dion P, Spiegelman D, McConkey BJ, Vande Velde C, Bouchard JP, Lacomblez L, Pochigaeva K, Salachas F, Pradat PF, Camu W, Meininger V, Dupre N, Rouleau GA. TARDBP mutations in individuals with sporadic and familial amyotrophic lateral sclerosis. Nat Genet 2008; 40: 572–574

Kasai T, Tokuda T, Ishigami N, Sasayama H, Foulds P, Mitchell DJ, Mann DMA, Allsop D, Nakagawa M. Increased TDP-43 protein in cerebrospinal fluid of patients with amyotrophic lateral sclerosis. Acta Neuropathol 2009; 117: 55–62

Kato M, Han TW, Xie S, Shi K, Du X, Wu LC, Mirzaei H, Goldsmith EJ, Longgood J, Pei J, Grishin NV, Frantz DE, Schneider JW, Chen S, Li L, Sawaya MR, Eisenberg D, Tycko R, McKnight SL. Cell-free Formation of RNA Granules: Low Complexity Sequence Domains Form Dynamic Fibers within Hydrogels. Cell 2012; 149: 753–767

Kawasaki T, Kawai T. Toll-Like Receptor Signaling Pathways. Front Immunol 2014; 5: 461

Kelley N, Jeltema D, Duan Y, He Y. The NLRP3 Inflammasome: An Overview of Mechanisms of Activation and Regulation. Int J Mol Sci 2019; 20: 3328

Kwiatkowski TJ Jr, Bosco DA, LeClerc AL, Tamrazian E, Vanderburg CR, Russ C, Davis A, Gilchrist J, Kasarskis EJ, Munsat T, Valdmanis P, Rouleau GA, Hosler BA, Cortelli P, Jong PJ de, Yoshinaga Y, Haines JL, Pericak-Vance MA, Yan J, Ticozzi N, Siddique T, McKenna-Yasek D, Sapp PC, Horvitz HR, Landers JE, Brown RH Jr. Mutations in the FUS/TLS Gene on Chromosome 16 Cause Familial Amyotrophic Lateral Sclerosis. Science 2009; 323:1205-8

Kwon HS, Koh SH. Neuroinflammation in neurodegenerative disorders: the roles of microglia and astrocytes. Transl Neurodegener 2020; 9: 42

Lagier-Tourenne C, Polymenidou M, Hutt KR, Vu AQ, Baughn M, Huelga SC, Clutario KM, Ling SC, Liang TY, Mazur C, Wancewicz E, Kim AS, Watt A, Freier S, Hicks GG, Donohue JP, Shiue L, Bennett CF, Ravits J, Cleveland DW, Yeo GW. Divergent roles of ALS-linked proteins FUS/TLS and TDP-43 intersect in processing long pre-mRNAs. Nat Neurosci 2012; 15: 1488–1497

Lattante S, Rouleau GA, Kabashi E. TARDBP and FUS Mutations Associated with Amyotrophic Lateral Sclerosis: Summary and Update. Hum Mutat 2013; 34: 812–826

Lee JC, Kim SJ, Hong S, Kim Y. Diagnosis of Alzheimer's disease utilizing amyloid and tau as fluid biomarkers. Exp Mol Med 2019; 51: 1–10

Lee KH, Zhang P, Kim HJ, Mitrea DM, Sarkar M, Freibaum BD, Cika J, Coughlin M, Messing J, Molliex A, Maxwell BA, Kim NC, Temirov J, Moore J, Kolaitis RM, Shaw TI, Bai B, Peng J, Kriwacki RW, Taylor JP. C9orf72 Dipeptide Repeats Impair the Assembly, Dynamics, and Function of Membrane-Less Organelles. Cell 2016; 167: 774-788.e17

Lepennetier G, Hracsko Z, Unger M, Van Griensven M, Grummel V, Krumbholz M, Berthele A, Hemmer B, Kowarik MC. Cytokine and immune cell profiling in the cerebrospinal fluid of patients with neuro-inflammatory diseases. J Neuroinflammation 2019; 16: 219

Li D, Wu M. Pattern recognition receptors in health and diseases. Signal Transduct Target Ther 2021; 6: 1–24

Li J, O W, Li W, Jiang ZG, Ghanbari HA. Oxidative Stress and Neurodegenerative Disorders. Int J Mol Sci 2013; 14: 24438–24475

Li YR, King OD, Shorter J, Gitler AD. Stress granules as crucibles of ALS pathogenesis. J Cell Biol 2013; 201: 361–372

Lippa CF, Rosso AL, Stutzbach LD, Neumann M, Lee VMY, Trojanowski JQ. Transactive response DNA-binding protein 43 burden in familial Alzheimer disease and Down syndrome. Arch Neurol 2009; 66: 1483–1488

Liscic RM, Alberici A, Cairns NJ, Romano M, Buratti E. From basic research to the clinic: innovative therapies for ALS and FTD in the pipeline. Mol Neurodegener 2020; 15: 31

Liu J, Wang F. Role of Neuroinflammation in Amyotrophic Lateral Sclerosis: Cellular Mechanisms and Therapeutic Implications. Front Immunol 2017; 8: 1005

Liu T, Zhang L, Joo D, Sun SC. NF-κB signaling in inflammation. Signal Transduct Target Ther 2017; 2: 17023

Logroscino G, Traynor BJ, Hardiman O, Chiò A, Mitchell D, Swingler RJ, Millul A, Benn E, Beghi E. Incidence of Amyotrophic Lateral Sclerosis in Europe. J Neurol Neurosurg Psychiatry 2010; 81: 385–390

Longinetti E, Fang F. Epidemiology of amyotrophic lateral sclerosis: an update of recent literature. Curr Opin Neurol 2019; 32: 771–776

Lu A, Magupalli VG, Ruan J, Yin Q, Atianand MK, Vos MR, Schröder GF, Fitzgerald KA, Wu H, Egelman EH. Unified Polymerization Mechanism for the Assembly of ASC-Dependent Inflammasomes. Cell 2014; 156: 1193–1206

Lu YC, Yeh WC, Ohashi PS. LPS/TLR4 signal transduction pathway. Cytokine 2008; 42: 145–151

Lučiūnaitė A, McManus RM, Jankunec M, Rácz I, Dansokho C, Dalgėdienė I, Schwartz S, Brosseron F, Heneka MT. Soluble Aβ oligomers and protofibrils induce NLRP3 inflammasome activation in microglia. J Neurochem 2020; 155: 650–661

Ludolph A, Petri S, Grosskreutz J. Motoneuronerkrankungen S1-Leitlinie 2021. In: Deutsche Gesellschaft für Neurologie, eds. Leitlinien für Diagnostik und Therapie in der Neurologie. Berlin: Deutsche Gesellschaft für Neurologie, 2021: 8-37

Lugrin J, Martinon F. Detection of ASC Oligomerization by Western Blotting. Bio Protoc 2017; 7: e2292

Mackenzie IRA. The Neuropathology of FTD Associated With ALS. Alzheimer Dis Assoc Disord 2007; 21: S44-49

Mamat U, Wilke K, Bramhill D, Schromm AB, Lindner B, Kohl TA, Corchero JL, Villaverde A, Schaffer L, Head SR, Souvignier C, Meredith TC, Woodard RW. Detoxifying Escherichia coli for endotoxin-free production of recombinant proteins. Microb Cell Fact 2015; 14: 57

Maniecka Z, Polymenidou M. From nucleation to widespread propagation: A prion-like concept for ALS. Virus Res 2015; 207: 94–105

Marchetti C, Swartzwelter B, Gamboni F, Neff CP, Richter K, Azam T, Carta S, Tengesdal I, Nemkov T, D'Alessandro A, Henry C, Jones GS, Goodrich SA, St. Laurent JP, Jones TM, Scribner CL, Barrow RB, Altman RD, Skouras DB, Gattorno M, Grau V, Janciauskiene S, Rubartelli A, Joosten LAB, Dinarello CA. OLT1177, a β-sulfonyl nitrile compound, safe in humans, inhibits the NLRP3 inflammasome and reverses the metabolic cost of inflammation. Proc Natl Acad Sci U S A 2018; 115: E1530–E1539

Marim FM, Silveira TN, Lima DS, Zamboni DS. A Method for Generation of Bone Marrow-Derived Macrophages from Cryopreserved Mouse Bone Marrow Cells. PLoS One 2010; 5: e15263

Masrori P, Van Damme P. Amyotrophic lateral sclerosis: a clinical review. Eur J Neurol 2020; 27: 1918–1929

Masumoto J, Taniguchi S, Ayukawa K, Sarvotham H, Kishino T, Niikawa N, Hidaka E, Katsuyama T, Higuchi T, Sagara J. ASC, a Novel 22-kDa Protein, Aggregates during Apoptosis of Human Promyelocytic Leukemia HL-60 Cells. J Biol Chem 1999; 274: 33835–33838

McKee CM, Coll RC. NLRP3 inflammasome priming: A riddle wrapped in a mystery inside an enigma. J Leukoc Biol 2020; 108: 937–952

Miller RG, Mitchell JD, Moore DH. Riluzole for amyotrophic lateral sclerosis (ALS)/motor neuron disease (MND). Cochrane Database Syst Rev 2012; 2012: CD001447

Moliner AM, Waligora J. The European Union Policy in the Field of Rare Diseases. Adv Exp Med Biol 2017; 1031: 561–587

Molliex A, Temirov J, Lee J, Coughlin M, Kanagaraj AP, Kim HJ, Mittag T, Taylor JP. Phase separation by low complexity domains promotes stress granule assembly and drives pathological fibrillization. Cell 2015; 163: 123–133

Mori K, Arzberger T, Grässer FA, Gijselinck I, May S, Rentzsch K, Weng S-M, Schludi MH, van der Zee J, Cruts M, Van Broeckhoven C, Kremmer E, Kretzschmar HA, Haass C, Edbauer D. Bidirectional transcripts of the expanded C9orf72 hexanucleotide repeat are translated into aggregating dipeptide repeat proteins. Acta Neuropathol 2013; 126: 881–893

Mukherjee S, Karmakar S, Babu SPS. TLR2 and TLR4 mediated host immune responses in major infectious diseases: a review. Braz J Infect Dis 2016; 20: 193–204

Muñoz-Planillo R, Kuffa P, Martínez-Colón G, Smith BL, Rajendiran TM, Núñez G. K^+ efflux is the common trigger of NLRP3 inflammasome activation by bacterial toxins and particulate matter. Immunity 2013; 38: 1142–1153

Nelson PT, Dickson DW, Trojanowski JQ, Jack CR, Boyle PA, Arfanakis K, Rademakers R, Alafuzoff I, Attems J, Brayne C, Coyle-Gilchrist ITS, Chui HC, Fardo DW, Flanagan ME, Halliday G, Hokkanen SRK, Hunter S, Jicha GA, Katsumata Y, Kawas CH, Keene CD, Kovacs GG, Kukull WA, Levey AI, Makkinejad N, Montine TJ, Murayama S, Murray ME, Nag S, Rissman RA, Seeley WW, Sperling RA, White III CL, Yu L, Schneider JA. Limbic-predominant age-related TDP-43 encephalopathy (LATE): consensus working group report. Brain 2019; 142: 1503–1527

Neumann M, Sampathu DM, Kwong LK, Truax AC, Micsenyi MC, Chou TT, Bruce J, Schuck T, Grossman M, Clark CM, McCluskey LF, Miller BL, Masliah E, Mackenzie IR, Feldman H, Feiden W, Kretzschmar HA, Trojanowski JQ, Lee VMY. Ubiquitinated TDP-43 in Frontotemporal Lobar Degeneration and Amyotrophic Lateral Sclerosis. Science 2006; 314: 130–133

Niedzielska E, Smaga I, Gawlik M, Moniczewski A, Stankowicz P, Pera J, Filip M. Oxidative Stress in Neurodegenerative Diseases. Mol Neurobiol 2016; 53: 4094–4125

Niu T, De Rosny C, Chautard S, Rey A, Patoli D, Groslambert M, Cosson C, Lagrange B, Zhang Z, Visvikis O, Hacot S, Hologne M, Walker O, Wong J, Wang P, Ricci R, Henry T, Boyer L, Petrilli V, Py BF. NLRP3 phosphorylation in its LRR domain critically regulates inflammasome assembly. Nat Commun 2021; 12: 5862

Nizami S, Millar V, Arunasalam K, Zarganes-Tzitzikas T, Brough D, Tresadern G, Brennan PE, Davis JB, Ebner D, Di Daniel E. A phenotypic high-content, high-throughput screen identifies inhibitors of NLRP3 inflammasome activation. Sci Rep 2021; 11: 15319

Nonaka T, Masuda-Suzukake M, Arai T, Hasegawa Y, Akatsu H, Obi T, Yoshida M, Murayama S, Mann DMA, Akiyama H, Hasegawa M. Prion-like Properties of Pathological TDP-43 Aggregates from Diseased Brains. Cell Rep 2013; 4: 124–134

Nzwalo H, de Abreu D, Swash M, Pinto S, de Carvalho M. Delayed diagnosis in ALS: the problem continues. J Neurol Sci 2014; 343: 173–175

Olson JK, Miller SD. Microglia Initiate Central Nervous System Innate and Adaptive Immune Responses through Multiple TLRs. J Immunol 2004; 173: 3916–3924

Olsson B, Lautner R, Andreasson U, Öhrfelt A, Portelius E, Bjerke M, Hölttä M, Rosén C, Olsson C, Strobel G, Wu E, Dakin K, Petzold M, Blennow K, Zetterberg H. CSF and blood biomarkers for the diagnosis of Alzheimer's disease: a systematic review and meta-analysis. Lancet Neurol 2016; 15: 673–684

Oskarsson B, Gendron TF, Staff NP. Amyotrophic Lateral Sclerosis: An Update for 2018. Mayo Clin Proc 2018; 93: 1617–1628

Péladeau C, Sandhu JK. Aberrant NLRP3 Inflammasome Activation Ignites the Fire of Inflammation in Neuromuscular Diseases. Int J Mol Sci 2021; 22: 6068

Peng Y, Chu S, Yang Y, Zhang Z, Pang Z, Chen N. Neuroinflammatory In Vitro Cell Culture Models and the Potential Applications for Neurological Disorders. Front Pharmacol 2021; 12: 671734

Petrov D, Mansfield C, Moussy A, Hermine O. ALS Clinical Trials Review: 20 Years of Failure. Are We Any Closer to Registering a New Treatment?. Front Aging Neurosci 2017; 9: 68

Pliner HA, Mann DM, Traynor BJ. Searching for Grendel: origin and global spread of the C9ORF72 repeat expansion. Acta Neuropathol 2014; 127: 391–396

Prasad A, Bharathi V, Sivalingam V, Girdhar A, Patel BK. Molecular Mechanisms of TDP-43 Misfolding and Pathology in Amyotrophic Lateral Sclerosis. Front Mol Neurosci 2019; 12: 25

Prell T, Grosskreutz J. The involvement of the cerebellum in amyotrophic lateral sclerosis. Amyotroph Lateral Scler Frontotemporal Degener 2013; 14: 507–515

Qin ZY, Gu X, Chen YL, Liu JB, Hou CX, Lin SY, Hao NN, Liang Y, Chen W, Meng HY. Toll-like receptor 4 activates the NLRP3 inflammasome pathway and periodontal inflam-maging by inhibiting Bmi-1 expression. Int J Mol Med 2021; 47: 137–150

Ren Y, Li S, Chen S, Sun X, Yang F, Wang H, Li M, Cui F, Huang X. TDP-43 and Phos-phorylated TDP-43 Levels in Paired Plasma and CSF Samples in Amyotrophic Lateral Sclerosis. Front Neurol 2021; 12: 663637

Renton AE, Majounie E, Waite A, Simón-Sánchez J, Rollinson S, Gibbs JR, Schymick JC, Laaksovirta H, van Swieten JC, Myllykangas L, Kalimo H, Paetau A, Abramzon Y, Remes AM, Kaganovich A, Scholz SW, Duckworth J, Ding J, Harmer DW, Hernandez DG, John-son JO, Mok K, Ryten M, Trabzuni D, Guerreiro RJ, Orrell RW, Neal J, Murray A, Pearson J, Jansen IE, Sondervan D, Seelaar H, Blake D, Young K, Halliwell N, Callister JB, Toul-son G, Richardson A, Gerhard A, Snowden J, Mann D, Neary D, Nalls MA, Peuralinna T, Jansson L, Isoviita VM, Kaivorinne AL, Hölttä-Vuori M, Ikonen E, Sulkava R, Benatar M, Wuu J, Chiò A, Restagno G, Borghero G, Sabatelli M, ITALSGEN Consortium, Hecker-man D, Rogaeva E, Zinman L, Rothstein JD, Sendtner M, Drepper C, Eichler EE, Alkan C, Abdullaev Z, Pack SD, Dutra A, Pak E, Hardy J, Singleton A, Williams NM, Heutink P, Pickering-Brown S, Morris HR, Tienari PJ, Traynor BJ. A hexanucleotide repeat expansion in C9ORF72 is the cause of chromosome 9p21-linked ALS-FTD. Neuron 2011; 72: 257–268

Ringholz GM, Appel SH, Bradshaw M, Cooke NA, Mosnik DM, Schulz PE. Prevalence and patterns of cognitive impairment in sporadic ALS. Neurology 2005; 65: 586–590

Rizzo FR, Musella A, De Vito F, Fresegna D, Bullitta S, Vanni V, Guadalupi L, Stampanoni Bassi M, Buttari F, Mandolesi G, Centonze D, Gentile A. Tumor Necrosis Factor and Interleukin-1β Modulate Synaptic Plasticity during Neuroinflammation. Neural Plast 2018; 2018: 8430123

Rosen DR, Siddique T, Patterson D, Figlewicz DA, Sapp P, Hentati A, Donaldson D, Goto J, O'Regan JP, Deng HX, Rahmani Z, Krizus A, McKenna-Yasek D, Cayabyab A, Gaston SM, Berger R, Tanzi RE, Halperin JJ, Herzfeldt B, Van den Bergh R, Hung WY, Bird T, Deng G, Mulder DW, Smyth C, Laing NG, Soriano E, Pericak–Vance MA, Haines J, Rouleau GA, Gusella JS, Horvitz HR, Brown RH. Mutations in Cu/Zn superoxide dismutase gene are associated with familial amyotrophic lateral sclerosis. Nature 1993; 362: 59–62

Ryan M, Heverin M, McLaughlin RL, Hardiman O. Lifetime Risk and Heritability of Amyotrophic Lateral Sclerosis. JAMA Neurol 2019; 76: 1367–1374

Sabogal-Guáqueta AM, Marmolejo-Garza A, de Pádua VP, Eggen B, Boddeke E, Dolga AM. Microglia alterations in neurodegenerative diseases and their modeling with human induced pluripotent stem cell and other platforms. Prog Neurobiol 2020; 190: 101805

Sameer AS, Nissar S. Toll-Like Receptors (TLRs): Structure, Functions, Signaling, and Role of Their Polymorphisms in Colorectal Cancer Susceptibility. Biomed Res Int 2021; 2021: 1157023

Sasaguri H, Chew J, Xu YF, Gendron TF, Garrett A, Lee CW, Jansen-West K, Bauer PO, Perkerson EA, Tong J, Stetler C, Zhang YJ. The extreme N-terminus of TDP-43 mediates the cytoplasmic aggregation of TDP-43 and associated toxicity in vivo. Brain Res 2016; 1647: 57–64

Sborgi L, Ravotti F, Dandey VP, Dick MS, Mazur A, Reckel S, Chami M, Scherer S, Huber M, Böckmann A, Egelman EH, Stahlberg H, Broz P, Meier BH, Hiller S. Structure and assembly of the mouse ASC inflammasome by combined NMR spectroscopy and cryo-electron microscopy. Proc Natl Acad Sci U S A 2015; 112: 13237–13242

Scheiblich H, Bousset L, Schwartz S, Griep A, Latz E, Melki R, Heneka MT. Microglial NLRP3 Inflammasome Activation upon TLR2 and TLR5 Ligation by Distinct α-Synuclein Assemblies. J Immunol 2021; 207: 2143–2154

Scheiblich H, Schlütter A, Golenbock DT, Latz E, Martinez-Martinez P, Heneka MT. Activation of the NLRP3 inflammasome in microglia: the role of ceramide. J Neurochem 2017; 143: 534–550

Schwarz H, Schmittner M, Duschl A, Horejs-Hoeck J. Residual Endotoxin Contaminations in Recombinant Proteins Are Sufficient to Activate Human CD1c+ Dendritic Cells. PLoS One 2014; 9: e113840

Spiller KJ, Restrepo CR, Khan T, Dominique MA, Fang TC, Canter RG, Roberts CJ, Miller KR, Ransohoff RM, Trojanowski JQ, Lee VMY. Microglia-mediated recovery from ALS-relevant motor neuron degeneration in a mouse model of TDP-43 proteinopathy. Nat Neurosci 2018; 21: 329–340

Sreedharan J, Blair IP, Tripathi VB, Hu X, Vance C, Rogelj B, Ackerley S, Durnall JC, Williams KL, Buratti E, Baralle F, de Belleroche J, Mitchell JD, Leigh PN, Al-Chalabi A, Miller CC, Nicholson G, Shaw CE. TDP-43 mutations in familial and sporadic amyotrophic lateral sclerosis. Science 2008; 319: 1668–1672

Strowig T, Henao-Mejia J, Elinav E, Flavell R. Inflammasomes in health and disease. Nature 2012; 481: 278–286

Stutz A, Horvath GL, Monks BG, Latz E. ASC speck formation as a readout for inflammasome activation. Methods Mol Biol 2013; 1040: 91–101

Swanson KV, Deng M, Ting JPY. The NLRP3 inflammasome: molecular activation and regulation to therapeutics. Nat Rev Immunol 2019; 19: 477–489

Talbott EO, Malek AM, Lacomis D. The epidemiology of amyotrophic lateral sclerosis. Handb Clin Neurol 2016; 138: 225–238

Tan RH, Ke YD, Ittner LM, Halliday GM. ALS/FTLD: experimental models and reality. Acta Neuropathol 2017; 133: 177–196

Taylor JP, Brown RH, Cleveland DW. Decoding ALS: from genes to mechanism. Nature 2016; 539: 197–206

Tejera D, Mercan D, Sanchez-Caro JM, Hanan M, Greenberg D, Soreq H, Latz E, Golenbock D, Heneka MT. Systemic inflammation impairs microglial Aβ clearance through NLRP3 inflammasome. EMBO J 2019; 38: e101064

Timmerman R, Burm SM, Bajramovic JJ. An Overview of in vitro Methods to Study Microglia. Front Cell Neurosci 2018; 12: 242

Uenal H, Rosenbohm A, Kufeldt J, Weydt P, Goder K, Ludolph A, Rothenbacher D, Nagel G. Incidence and Geographical Variation of Amyotrophic Lateral Sclerosis (ALS) in Southern Germany – Completeness of the ALS Registry Swabia. PLoS One 2014; 9: e93932

Vance C, Rogelj B, Hortobágyi T, De Vos KJ, Nishimura AL, Sreedharan J, Hu X, Smith B, Ruddy D, Wright P, Ganesalingam J, Williams KL, Tripathi V, Al-Saraj S, Al-Chalabi A, Leigh PN, Blair IP, Nicholson G, de Belleroche J, Gallo JM, Miller CC, Shaw CE. Mutations in FUS, an RNA Processing Protein, Cause Familial Amyotrophic Lateral Sclerosis Type 6. Science 2009; 323: 1208–1211

Verber N, Shaw PJ. Biomarkers in amyotrophic lateral sclerosis: a review of new developments. Curr Opin Neurol 2020; 33: 662–668

Verstraete E, Kuiperij HB, van Blitterswijk MM, Veldink JH, Schelhaas HJ, van den Berg LH, Verbeek MM. TDP-43 plasma levels are higher in amyotrophic lateral sclerosis. Amyotroph Lateral Scler 2012; 13: 446–451

Vidya MK, Kumar VG, Sejian V, Bagath M, Krishnan G, Bhatta R. Toll-like receptors: Significance, ligands, signaling pathways, and functions in mammals. Int Rev Immunol 2018; 37: 20–36

Voet S, Srinivasan S, Lamkanfi M, van Loo G. Inflammasomes in neuroinflammatory and neurodegenerative diseases. EMBO Mol Med 2019; 11: e10248

Vu LT, Bowser R. Fluid-Based Biomarkers for Amyotrophic Lateral Sclerosis. Neurotherapeutics 2017; 14: 119–134

Wakelin SJ, Sabroe I, Gregory CD, Poxton IR, Forsythe JLR, Garden OJ, Howie SEM. "Dirty little secrets"—Endotoxin contamination of recombinant proteins. Immunol Lett 2006; 106: 1–7

Walker AK, Spiller KJ, Ge G, Zheng A, Xu Y, Zhou M, Tripathy K, Kwong LK, Trojanowski JQ, Lee VMY. Functional recovery in new mouse models of ALS/FTLD after clearance of pathological cytoplasmic TDP-43. Acta Neuropathol 2015; 130: 643–660

Walker LC, Diamond MI, Duff KE, Hyman BT. Mechanisms of Protein Seeding in Neuro-degenerative Diseases. JAMA Neurol 2013; 70: 304-310

Writing Group, Edaravone (MCI-186) ALS 19 Study Group. Safety and efficacy of edara-vone in well defined patients with amyotrophic lateral sclerosis: a randomised, double-blind, placebo-controlled trial. Lancet Neurol 2017; 16: 505–512

Yedavalli VS, Patil A, Shah P. Amyotrophic Lateral Sclerosis and its Mimics/Variants: A Comprehensive Review. J Clin Imaging Sci 2018; 8: 53

Yu L, Wang L, Chen S. Endogenous toll-like receptor ligands and their biological signifi-cance. J Cell Mol Med 2010; 14: 2592–2603

Zanoni I, Ostuni R, Marek LR, Barresi S, Barbalat R, Barton GM, Granucci F, Kagan JC. CD14 controls the LPS-induced endocytosis of Toll-like Receptor 4. Cell 2011; 147: 868–880

Zhao W, Beers DR, Bell S, Wang J, Wen S, Baloh RH, Appel SH. TDP-43 activates mi-croglia through NF-κB and NLRP3 inflammasome. Exp Neurol 2015; 273: 24–35

Zito G, Buscetta M, Cimino M, Dino P, Bucchieri F, Cipollina C. Cellular Models and As-says to Study NLRP3 Inflammasome Biology. Int J Mol Sci 2020; 21: 4294

Zu T, Gibbens B, Doty NS, Gomes-Pereira M, Huguet A, Stone MD, Margolis J, Peterson M, Markowski TW, Ingram MAC, Nan Z, Forster C, Low WC, Schoser B, Somia NV, Clark HB, Schmechel S, Bitterman PB, Gourdon G, Swanson MS, Moseley M, Ranum LPW. Non-ATG–initiated translation directed by microsatellite expansions. Proc Natl Acad Sci U S A 2011; 108: 260–265

9. Acknowledgements